RESEARCH ARTICLE



Differential investment in brain regions for a diurnal and nocturnal lifestyle in Australian Myrmecia ants

Zachary B. V. Sheehan¹ | J. Frances Kamhi¹ | Marc A. Seid^{1,2} | Ajay Narendra¹

¹Department of Biological Sciences, Macquarie University, Sydney, New South Wales, Australia

²Biology Department, Neuroscience Program, The University of Scranton, Scranton, Pennsylvania

Correspondence

Department of Biological Sciences, Macquarie University, 205 Culloden Road, Sydney, NSW

Email: ajay.narendra@mq.edu.au

Funding information

Australian Research Council, Grant/Award Numbers: DP150101172, FT140100221

Abstract

Animals are active at different times of the day. Each temporal niche offers a unique light environment, which affects the quality of the available visual information. To access reliable visual signals in dim-light environments, insects have evolved several visual adaptations to enhance their optical sensitivity. The extent to which these adaptations reflect on the sensory processing and integration capabilities within the brain of a nocturnal insect is unknown. To address this, we analyzed brain organization in congeneric species of the Australian bull ant, Myrmecia, that rely predominantly on visual information and range from being strictly diurnal to strictly nocturnal. Weighing brains and optic lobes of seven Myrmecia species, showed that after controlling for body mass, the brain mass was not significantly different between diurnal and nocturnal ants. However, the optic lobe mass, after controlling for central brain mass, differed between day- and night-active ants. Detailed volumetric analyses showed that the nocturnal ants invested relatively less in the primary visual processing regions but relatively more in both the primary olfactory processing regions and in the integration centers of visual and olfactory sensory information. We discuss how the temporal niche occupied by each species may affect cognitive demands, thus shaping brain organization among insects active in dim-light conditions.

allometric scaling, ants, brain, Myrmecia, neuropil, RRID:AB_2315424, RRID:AB_2535771, RRID:SCR_002285, RRID:SCR_007353, temporal niche

1 | INTRODUCTION

Vision is a crucial sensory modality for most animals. Visual information is used to track prey, find mates, avoid predators, regulate daily activity rhythms, and navigate between places of significance (Collett & Zeil, 2018; Cronin, Johnsen, Marshall, & Warrant, 2014; Heinze, Narendra, & Cheung, 2018). In dim-light conditions the visual signal-to-noise ratio is low, which dramatically affects the availability and the salience of visual cues (Narendra, Kamhi, & Ogawa, 2017; Warrant, 2017). Indeed, on moonless nights, light levels can decrease by up to 11 orders of magnitude compared to a cloudless day (O'Carroll & Warrant, 2017), making it a challenge to access reliable visual information. Nevertheless, animals active in low light environments use visual information for navigation (Narendra et al., 2017;

This article was published online on 22 January 2019. An error was subsequently identified. This notice is included in the online and print versions to indicate that both have been corrected 11 February 2019.

Warrant & Dacke, 2011). To access reliable visual information in dim light, the most extreme form of optical adaptation is found in the optical superposition eyes of crustaceans and insects (Land & Fernald, 1992; Land & Nilsson, 2012). However, some subtle adaptations are found in insects that have an apposition type of compound eye (e.g., ants, bees, wasps), an eye design that is best suited for high light levels. These insects modify their apposition compound eyes by developing larger lenses and wider rhabdoms leading to a 27-30-fold increase in their optical sensitivity (Greiner, 2006; Greiner et al., 2007; Narendra et al., 2011; Somanathan, Kelber, Borges, Wallen, & Warrant, 2009; Warrant, 2008; Warrant & Dacke, 2011).

This increase in optical sensitivity, though significant, is not sufficient to explain the visually guided behaviors of insects at low light levels (Warrant, 2008). Insects may thus engage in spatial and temporal integration of receptor signals to improve the visual signal-to-noise ratio at low light levels (Greiner, Ribi, & Warrant, 2005; Stöckl, O'Carroll, & Warrant, 2016; Warrant, 2017). Spatial summation is thought to occur in the first optic neuropil, the lamina, via extensive lateral branching of laminar

monopolar cell dendrites into neighboring cartridges, which receive input from single ommatidia (Greiner, Ribi, Wcislo, & Warrant, 2004; Ribi, 1975; Stöckl, Ribi, & Warrant, 2016). Apart from these adaptations found in the peripheral sensory system, it is unclear whether and how the size of distinct brain regions changes between visually oriented day- and night-active animals. To the best of our knowledge, neuropil investment patterns in nocturnal insects have been investigated only in hawkmoths (Stöckl, Heinze, et al., 2016), sphinx moths (El Jundi, Huetteroth, Kurylas, & Schachtner, 2009) and wasps (O'Donnell et al., 2013; O'Donnell & Bulova, 2017). All of these nocturnal insects invested more in their antennal lobes compared to the optic lobes, suggesting nocturnal insects relied more on olfactory information. This neuropil investment pattern nicely aligns to the animals' sensory ecologies, and was most evident in the nocturnal hawkmoths that relied more strongly on olfactory cues than the diurnal species (Stöckl, Heinze, et al., 2016). A comparison of butterfly and moth brains (Heinze & Reppert, 2012; El Jundi, et al., 2009; Montgomery & Ott, 2015) showed that diurnal butterflies that occupy shaded habitats invested more in their olfactory system and had a brain organization that more closely resembled the nocturnal moths than the diurnal monarch butterfly. Investment patterns into different neuropils have also been investigated in locusts where the crepuscular species had larger primary sensory neuropils, for both vision and olfaction, whereas the diurnal species invested more into the mid brain (Ott & Rogers, 2010). However, this differential investment pattern in locusts has been attributed to their lifestyles of being solitary or gregarious, instead of time of activity.

Here, we aim to identify the investment patterns of functionally distinct brain regions in congeneric day- and night-active ants that rely predominantly on visual information. We studied a set of closely related species of the Australian ant genus Myrmecia (i.e., bull ants, jack jumpers, or inch ants) that almost exclusively depend on visual information for above-ground activity irrespective of their time of activity (Eriksson, 1985; Freas, Narendra, Lemesle, & Cheng, 2017; Freas, Wystrach, Narendra, & Cheng, 2018; Narendra, Gourmaud, & Zeil, 2013; Narendra & Ramirez-Esquivel, 2017; Narendra, Reid, & Hemmi, 2010; Narendra, Reid, & Raderschall, 2013). Closely related species of this genus have evolved distinct visual adaptations to occupy their respective light environments (Greiner et al., 2007; Narendra et al., 2011; Narendra & Ribi, 2017). However, although ant brains have been well-characterized and functionally distinct brain regions are known to change with size, morphologically distinct subcaste, age and experience (Bressan et al., 2015; Ehmer & Gronenberg, 2004; Gronenberg, Heeren, & Hölldobler, 1996; Kamhi, Sandridge-Gresko, Walker, Robson, & Traniello, 2017; Muscedere, Gronenberg, Moreau, & Traniello, 2014; Muscedere & Traniello, 2012; Stieb, Muenz, Wehner, & Rössler, 2010), how brains of nocturnal ants adapt to dim-light conditions has never been investigated. The only study that addressed a slightly similar question compared brains of army ants that foraged above ground (likely to experience bright light conditions) to those that were subterranean (likely to experience dim-light conditions), where the above-ground foragers invested more into visual processing regions (Bulova, Purce, Khodak, Sulger, & O'Donnell, 2016). Here, we first provide an overview of the scaling patterns of optic lobes across several diurnal and nocturnal Myrmecia ants. We then present a detailed scaling analysis of functionally distinct brain regions in a strictly day-active and night-active *Myrmecia* species to identify how brain component size is tuned to specific temporal niche.

2 | MATERIALS AND METHODS

2.1 | Scaling patterns of brain and optic lobe weights

We collected seven species of Myrmecia ants (Figure 1) from multiple nests in Sydney and Canberra, Australia. This included four day-active species: Myrmecia croslandi (35°14′43.69″S, 149°10′06.33″E), Myrmecia gulosa (33°37′46.35″S, 150°46′04.47″E), Myrmecia nigrocincta (33°37′46.35″S, 150°46′04.47″E), Myrmecia tarsata (33°46′10.11″S, 151°06′26.57″E) and three night-active species: Myrmecia midas (33°46'10.24"S, 151°06′39.55″E), Myrmecia nigriceps (35°14′43.69″S, 149°10′06.33″E) and Myrmecia pyriformis (35°14'43.69"S, 149°10'06.33"E). Five of these (M. gulosa, M. tarsata, M. midas, M. nigriceps, M. pyriformis) belong to the gulosa species group, M. croslandi belongs to the pilosula species group and M. nigrocincta belongs to the nigrocincta species group (Hasegawa & Crozier, 2006; Ogata, 1991; Ogata & Taylor, 1991). The activity schedules of six of the above seven Myrmecia species have been described previously (Freas, Narendra, & Cheng, 2017; Greiner et al., 2007; Narendra et al., 2010). We determined the activity pattern of the remaining species, M. gulosa, by monitoring worker activity at one colony on April 27, 2017 at the collection site. We set up a 60-cm perimeter around the nest entrance and observed the time of entry and exit of individual ants over a 24 hr period on a single cloud-free day (Figure 2a). Astronomical data on sunrise, sunset, and astronomical twilight times were obtained from Geoscience Australia (http://www.ga.gov.au). The start of astronomical twilight is defined as the instant in the morning when the center of the Sun is at a depression angle of 18° below an ideal horizon and similarly, the end of astronomical twilight is in the evening when the center of the Sun is at a depression angle of 18° below an ideal horizon (Narendra et al., 2010). At low light, we used a head lamp with a red filter to observe ants and this did not appear to affect their behavior.

Myrmecia ants exhibit distinct body size variation both within and between species. Hence, we first determined the body mass of each ant. For this, we anesthetized ants individually by placing them in an icebox for 10–15 min to cool them down and then weighed them using a micro balance (Sartorius CPA2P, Gottingen, Germany, RRID: SCR_003880). Following this, the brains were quickly dissected. For detailed methods, see Seid, Castillo, and Wcislo (2011). Photoreceptors of both eyes were removed, and the brains were weighed. To assess the contribution of the optic lobe, we carefully separated the optic lobes from the central brain and weighed either the left or the right one. Such a dissection was possible due to the relatively large optic lobes in Myrmecia ants. To minimize desiccation, the tissue was first placed within a small droplet of Ringer's solution and weighed within 4 s of the droplet being wicked away using a Kimwipe[®].

2.2 | Immunocytochemistry

We identified the scaling relationships of functionally distinct brain regions in the day-active *M. gulosa* and the night-active *M. midas*. There was significant intra-species size variation in both species (head

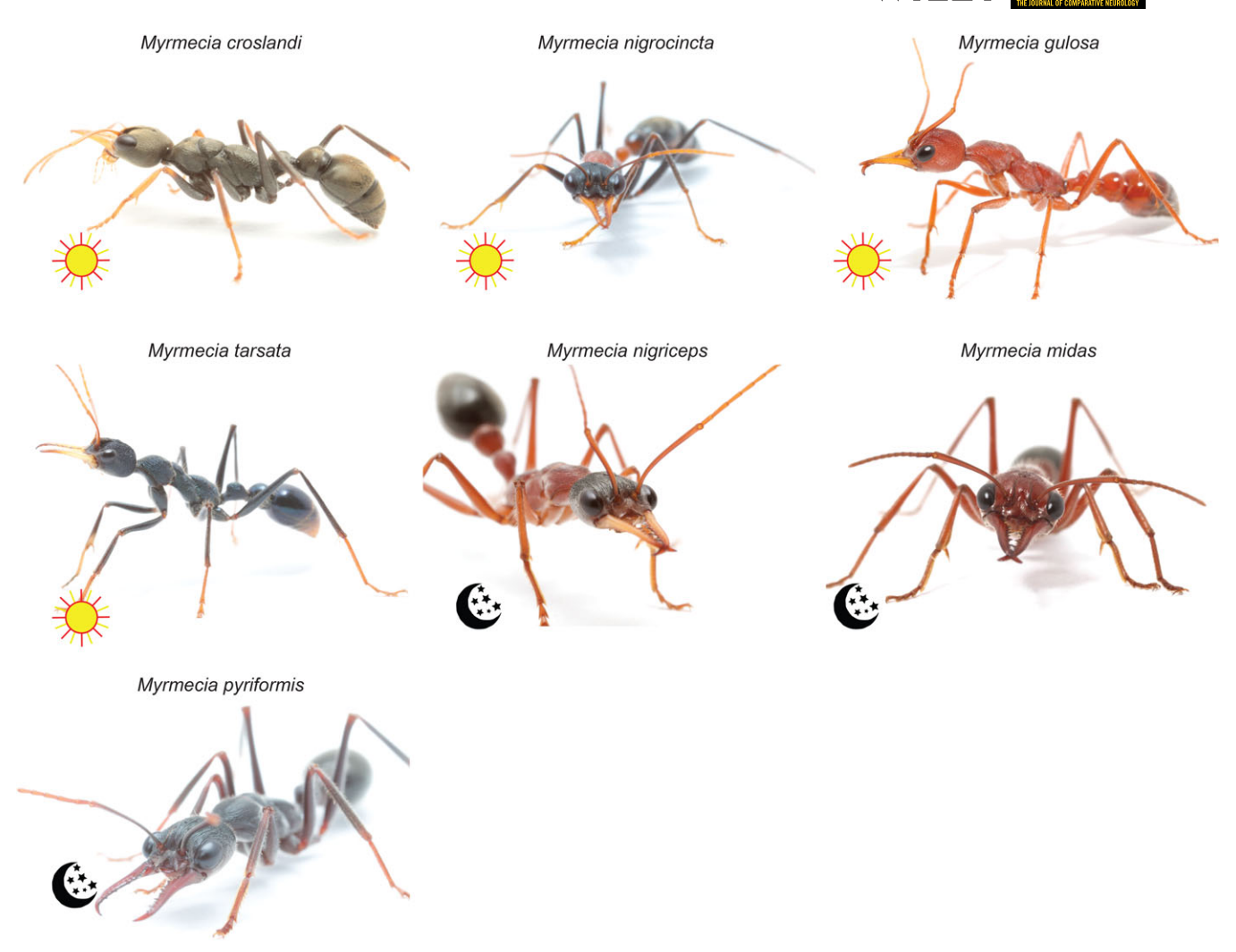


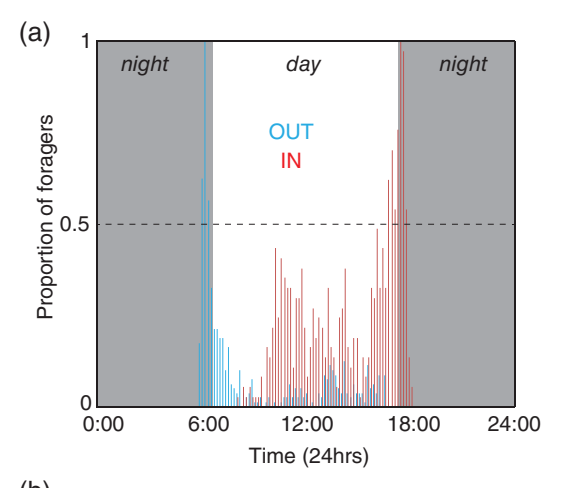
FIGURE 1 Congeneric species of *Myrmecia* that are active at different times of the day. Day-active species (sun): *Myrmecia croslandi*, *Myrmecia nigrocincta*, *Myrmecia gulosa*, *Myrmecia tarsata*. Night-active species (moon): *Myrmecia nigriceps*, *Myrmecia midas* and *Myrmecia pyriformis*. Daily worker activity patterns of *M. gulosa* are shown in Figure 2 and activity pattern of the other species have been described previously (Freas, Narendra, & Cheng, 2017; Greiner et al., 2007; Narendra et al., 2010) [Color figure can be viewed at wileyonlinelibrary.com]

width of *M. gulosa*: 1.9-4.0 mm; *M. midas*: 2.1-4.5 mm; Figure 2b, light shade). We measured brain volumes from 30 individuals in both species spanning most of the body size variation (Figure 2b, dark shade).

Animals were cooled on ice and their dorsal head surface was photographed with a color camera (Lumix DMC-FZ1000, Panasonic Australia). From these images, the head width (HW) of each ant was measured along the widest point of the head, which was directly behind the eyes. Brains were dissected in physiological saline solution (129 mM NaCL, 6 mM KCl, 4.3 mM MgCl $_2 \times$ 6H $_2$ O, 5 mM CaCl $_2 \times$ 2 H₂O, 159.8 mM Sucrose, 274 mM D-glucose, 10 mM HEPES buffer, pH 6.7) and transferred into a fixative solution (4% paraformaldehyde [PFA] in phosphate buffered saline [PBS]) within 10 min. We followed a modified protocol (Groh, Lu, Meinertzhagen, & Rössler, 2012; Kamhi, Gronenberg, Robson, & Traniello, 2016) for antibody staining for whole-mount brains. Brains were kept on a shaker for all washes and incubations. Brains were kept in the fixative at room temperature for 2 days and then washed in PBS (3 \times 10 min) at room temperature. To facilitate antibody penetration, they were then washed with 3% Triton-X in PBS (PBST; 3×10 min) at room temperature. Brains were

then preincubated at room temperature for 1 hr with 2% Normal Goat Serum (NGS, Sigma-Aldrich) in PBST. Samples were then incubated for 4 days at room temperature in the primary antibody solution (1:50 anti-synapsin [3C11 anti-SYNORF1; DHSB, RRIS:AB 2315424; Table 1], 2% NGS in PBST) on a shaker. After further washes in PBS (5 \times 10 min), specimens were incubated in the dark for 3 days at room temperature in the secondary antibody solution (1:250 Alexa Fluor 488 goat antimouse [ThermoFisher Scientific, RRID:AB_2535771], 1% NGS in PBST). This was followed by PBS washes (5 \times 10 min) and dehydration through an ascending ethanol series (30%, 50%, 70%, 90%, 95%, 100%, 100%; 10 min each). Brains were first cleared for 10 min in 1:1 ethanol:methyl salicylate followed by 100% methyl salicylate for 1 hr at room temperature. Brains were then transferred to custom-made metal slides with 1 cm diameter holes sealed on one side by gluing a coverslip to create a well. In these wells, brains were immersed in 100% methyl salicylate with the ventral side facing upward and sealed with a coverslip.

The brains were imaged with an inverted confocal laser scanning microscope (Olympus FluoView FV1000© IX81) using a 10x objective (UPlanApo, NA 0.4) and 3.1 μ m optical sections. We used the



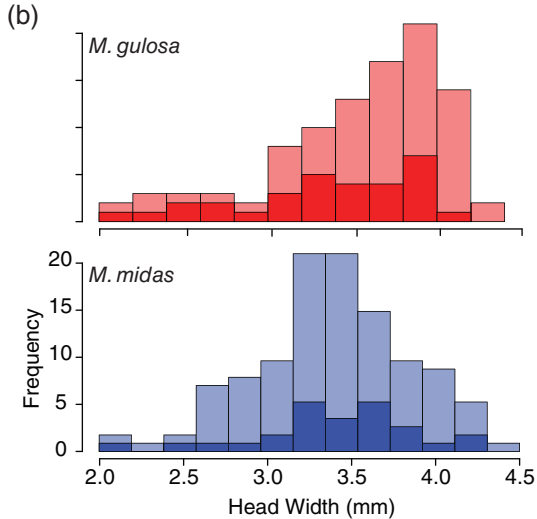


FIGURE 2 Daily activity schedule and body size variation of Myrmecia ants. (a) Daily activity schedule of Myrmecia gulosa recorded on a single day (April 20, 2017) indicating the proportion of ants that exited (blue) and returned to the nest (red). The proportion of foragers is normalized to the maximum number of foragers leaving or returning to the nest. Dark shaded region is night and white region is day. (b, c) Head width variation in day-active Myrmecia gulosa (red) and night-active Myrmecia midas (blue). Frequency distribution of head widths of ants in a colony is shown in a lighter shade, and the frequency distribution of head widths in which the brains were studied is shown in a darker color [Color figure can be viewed at wileyonlinelibrary.com]

software Amira (v. 6.0.1, ThermoFisher Scientific, RRID:SCR_007353) to trace functionally distinct neuropils, to both obtain volumetric measurements and create 3D reconstructions. Using Amira's segmentation editor, we manually outlined individual neuropils based on the anti-

TABLE 1 Primary antibodies

Antigen	Immunogen	Source	Dilution
Synapsin	Fusion protein of glutathione S- transferase and the Drosophila SYN1 protein	Developed by E Buchner (University of Würzburg, Germany) obtained from DSHB, University of Iowa; mouse, monoclonal; Cat #3C11 (anti SNYORF1); RRID: AB_528479	1:50

synapsin staining and used the "Interpolate" function to create a complete representation of these neuropils. To account for differences in refractive indices, the "z axis" was corrected by multiplying the optical section thickness by 1.581 (Bucher, Scholz, Stetter, Obermayer, & Pflüger, 2000; Hell, Reiner, Cremer, & Stelzer, 1993). Neuropil volumes were calculated from the outlined neuropils using the "MaterialStatistics" function of Amira. The following well-defined neuropil regions in the ant brain were quantified (Figure 3): the antennal lobes (AL), mushroom bodies (MB; containing the calyx lip [CA-Lip], calyx collar [CA-Col] and peduncle and lobes [PED+L]), the optic lobes (OL; containing the lamina [LA], medulla [ME] and lobula [LO]), the central complex (CX; containing the central body upper unit [CBU], the central body lower unit [CBL], the noduli [NO] and the protocerebral bridge [PB]), the subesophageal zone (SEZ), and the rest of the central brain (RoCB). Cell bodies were not included in these measurements. The volume of the anterior optic tubercle, an important part of the visual processing circuitry, was not measured here due to poorly defined borders in the ant brain.

Due to the large size of the bull ant brain, three overlapping z-stacks were imaged: one of the central brain and one on either side of the central brain. For 3D-resconstructions these three image stacks were merged together into a single image using the "Pairwise Stitching" plugin in the program Fiji (Schindelin et al., 2012; RRID: SCR_02285). 3D reconstructions were created using a polygonal surface model in Amira.

2.3 | Data analysis

Brain weights: We used a linear mixed effects model to analyze the allometric relationships between (a) brain weight and body weight, and (b) optic lobe weight and central brain weight. We used the R package "Ime4" with the restricted maximum likelihood (REML) estimation method to build the models. All weight measures were log transformed. To examine whether body weight was related to activity time we regressed log-transformed body weight over activity time (fixed effect) using a mixed effects model, with species as the random effect. To investigate how brain weight changed with body weight in diurnal and nocturnal species, we used a mixed effect model to predict brain weight and optic lobe weight. Body weight or central brain weight and activity time (diurnal or nocturnal) were included as fixed effects and species as the random effect. The interaction between body weight or central brain weight and activity time was included as fixed effect in the full model. Interaction terms that were not significant at p < .05 were removed to generate a reduced model. We report the coefficients, standard errors and p-values of both the full and reduced models.

We show the relationship between log body weight and log brain weight as a scatterplot. We also show regression lines for each species using intercepts and slopes derived from mixed models. For this, brain weight was regressed over body weight as fixed effect and species as random effect. Similarly, we show a scatterplot to visualize the relation between weight of the optic lobes and central brain along with mixed model derived species-specific regression lines.

Brain volumes: For all paired neuropils, we traced one hemisphere of the brain and multiplied the volume of each paired neuropil by two to obtain an estimate of the volume of the entire bilateral neuropil

1265

(Kamhi et al., 2016). Summing the volume of all paired and unpaired neuropils provided the total neuropil volume of the brain. The volume of all the neuropils together with the cell rind provided the volume of the entire brain. We combined the data from multiple nests because we did not find any nest effect for major neuropils for either species (Linear model: antennal lobe: M. gulosa: $F_{4,29}$ = 2.483, p = .126; M. midas: $F_{4,26} = 1.777$, p = .194; optic lobe: M. gulosa: $F_{4.29} = 0.3287$, p = .5709; M. midas: $F_{4.26} = 3.961$, p = .057; mushroom body: M. gulosa: $F_{4,29} = 2.089$, p = .159; M. midas: $F_{4,26} = 3.798$, p = .06; central complex: M. gulosa: $F_{4.29} = 1.612$, p = .214; M. midas: $F_{4,26}$ = 0.6254, p = .4362). The volumes of the CX, SEZ, and RoCB did not differ between the two species (see results) and we used the sum of their volumes as a "reference structure" to compare the volume of

each brain region (except CX and SEZ). To describe the scaling patterns of CX (and its subregions) and SEZ, we used the volume of SEZ + RoCB and CX + RoCB, respectively, as the 'reference structure'. We carried out the scaling analysis using a standardized major axis (SMA) regression in the statistical package (S)MATR v.3.4 for R (Warton, Wright, Falster, & Westoby, 2006). If the slopes between species were not statistically different, we tested for differences in the elevation, along the y axis, which indicates difference between species. All variables were natural log-transformed before scaling analyses. We used a grade shift index (gsi) to estimate how much larger each brain region was in a day-active species compared to the nightactive species for a given body size: $gsi = e^{\alpha \text{ diurnal}-\alpha \text{ nocturnal}}$. as described in Ott and Rogers (2010).

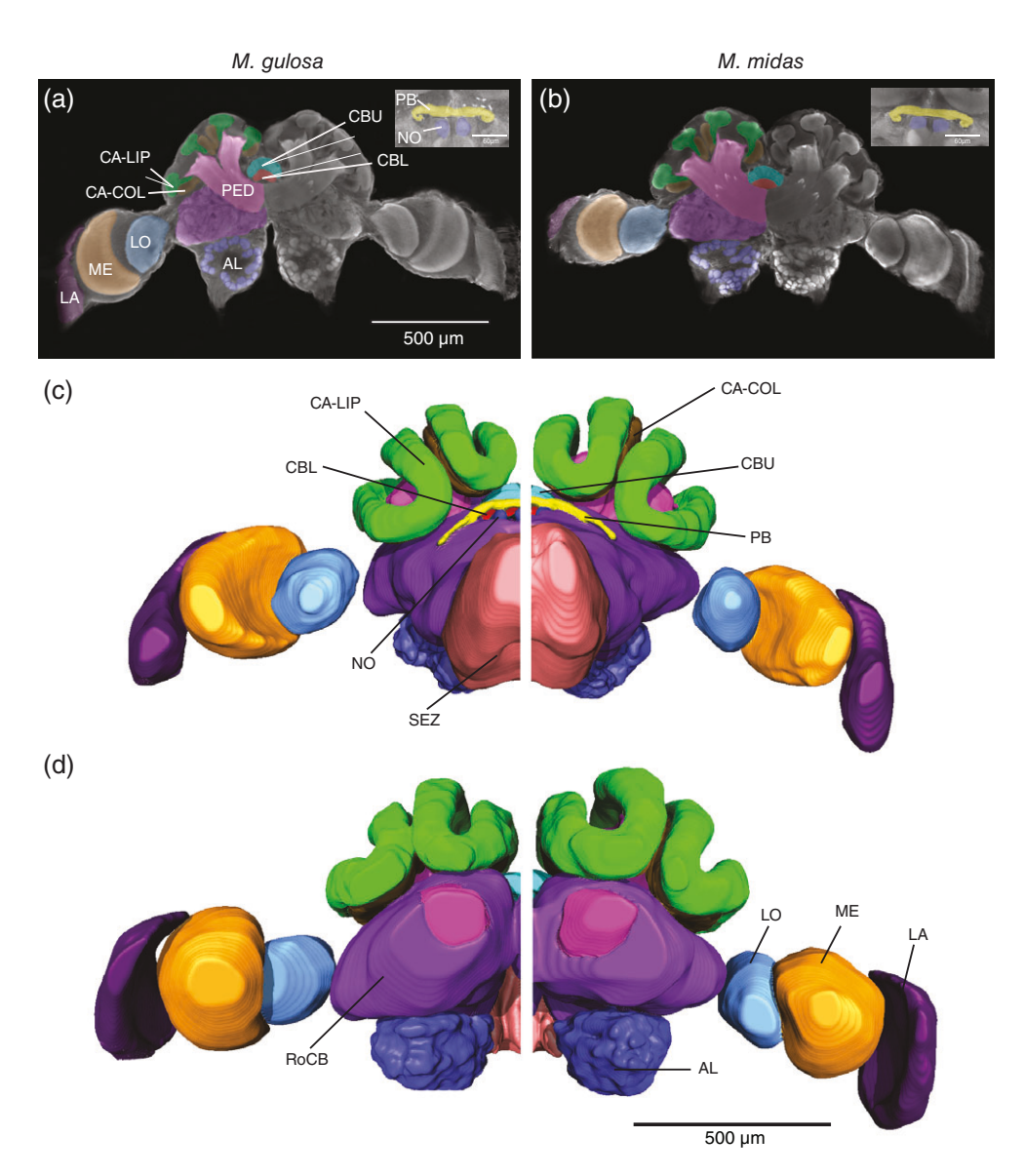


FIGURE 3 Organization of brain neuropils in a day-active (Myrmecia gulosa, left) and night-active ant (Myrmecia midas, right). (a, b) Horizontal section of the brain labelled with synapsin. Colorized regions on one half of the brain depict the neuropils traced in this study. Inset: Protocerebral bridge (PB) and noduli (NO). (c, d) 3D reconstruction of the neuropils of two individual ants of comparable head widths. (c) Dorsal and (d) ventral views of each species showing: LA = lamina; ME = medulla; LO = lobula; AL = antennal lobe; CA-LIP = mushroom body calyx lip; CA-COL = mushroom body calyx collar; PED = peduncle; CBU = central body upper unit; CBL = central body lower unit; NO = noduli; PB = protocerebral bridge; SEZ = subesophageal zone. The rest of the central brain region is indicated as RoCB. Scale for (a) and (b) are shown in panel a; scale for (c) and (d) are shown in panel d [Color figure can be viewed at wileyonlinelibrary.com]

3 | RESULTS

3.1 | Activity schedule

The activity schedule of all the *Myrmecia* species, except *M. gulosa*, have been previously described. Workers of *M. gulosa* were mostly day-active (Figure 2a). The majority of the ants left the nest during the morning twilight, between 5 and 10 min before sunrise. Activity at the nest continued throughout the day and a majority of the animals returned home during the evening twilight, about 10–20 min after sunset.

3.2 | Scaling patterns of brain and optic lobe mass

Two of the day-active species, M. croslandi and M. nigrocincta had the smallest body size and they also had the smallest brains (Figure 4a; Table 2). Body weight was not significantly associated with time of activity in the seven Myrmecia ant species (linear mixed model: estimate: 0.663; SE: 0.3805, p = .142). As evident from Figure 4a, brain weight increased with body weight across all species. After controlling for body weight, we found that brain weight was not significantly different between day- and night-active species (Figure 4a; reduced model in Table 3). In contrast, after controlling for central brain weight, optic lobe weight was significantly different between the day- and night-active species (Figure 4b; reduced model in Table 3).

3.3 | Volumetric analysis of brain regions

3.3.1 | Relative investment in peripheral sensory neuropils

The optic lobe is the first visual processing unit. Relative to the volume of the reference structure (CX + SEZ + RoCB), the optic lobes were larger in the day-active species compared to the night-active species (Figure 5; Tables 4 and 5). The optic lobe consists of three neuropils. The first neuropil, the lamina, was relatively large in the day-active species (Table 5). A similar pattern was found in the medulla. However for the lobula, the

scaling slopes of the two groups were significantly different, (Table 5) which made it theoretically invalid to test for a grade shift. The antennal lobe is the first olfactory processing unit. Relative to the reference structure, the antennal lobes were larger in the nocturnal ants compared to the day-active ants (Figure 6, Table 5).

3.3.2 | Relative investment of higher order sensory neuropils

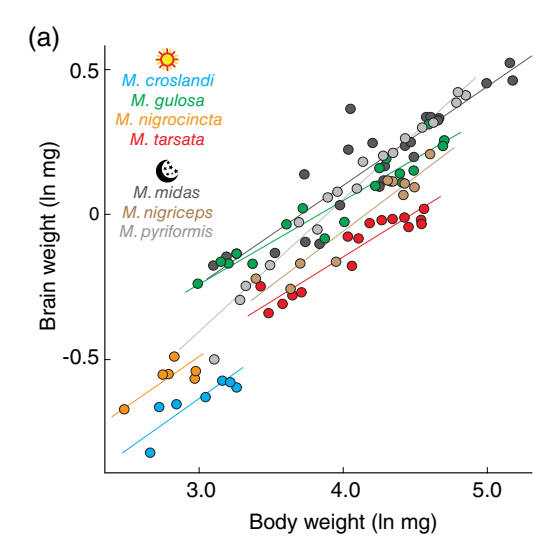
Relative to the reference structure (CX + SEZ + RoCB), the volume of the mushroom body was larger in the nocturnal *M. midas* compared to the diurnal *M. gulosa* (Figure 7, Table 5). All the sub-regions of the mushroom body were relatively larger in the nocturnal ants compared to the diurnal ants. The volume of the central complex did not differ between the day- and night-active ants (Figure 8). Such a pattern was seen in most of the sub-regions of the central complex: the central body upper unit, the noduli, and protocerebral bridge. The central body lower unit was the only sub-region of the central complex that was larger in the day-active ants compared to the night-active species.

3.3.3 | Relative investment in the SEZ

Relative to the reference structure (CX + RoCB), the SEZ, which is involved in controlling the mandibles and mouthparts, did not differ between the day- and night-active species (Table 5).

4 | DISCUSSION

To determine how brains adapt to different light environments, we measured brain mass and neuropil volume in congeneric species of *Myrmecia* ants that rely extensively on visual information (Freas, Narendra, Lemesle, & Cheng, 2017; Narendra, Gourmaud, & Zeil, 2013; Narendra, Reid, & Raderschall, 2013; Reid, Narendra, Hemmi, & Zeil, 2011). We show that brain region investment varies systematically between diurnal and nocturnal species. Nocturnal ants have evolved distinct adaptations that may enhance their visual and olfactory



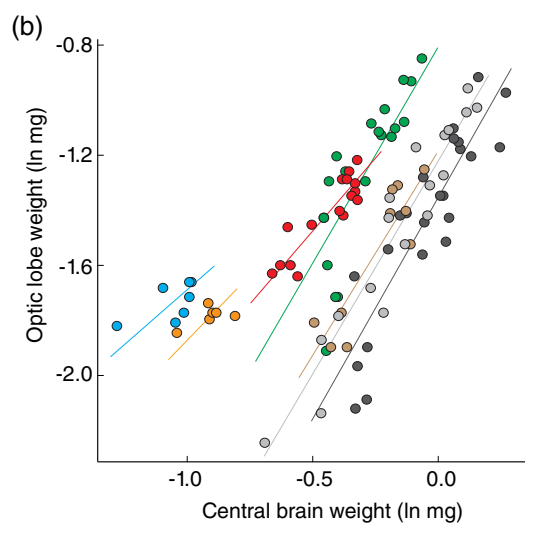


FIGURE 4 Relationship between optic lobe, brain, and body weights in diurnal and nocturnal *Myrmecia* ants. Scaling pattern of (a) brain mass to body weight, and (b) optic lobes weight to central brain weight in 4 day-active and 3 night-active *Myrmecia* species. Species are color coded and the day-(sun) and night-active (moon) species are indicated. Each dot represents one individual. Species-specific regression lines are based on intercepts and slopes derived from linear mixed models (see methods) [Color figure can be viewed at wileyonlinelibrary.com]

TABLE 2 Weights of body, brain and optic lobes in seven species of Myrmecia ants. Day-active: Myrmecia croslandi (n = 7), Myrmecia gulosa (n = 20), Myrmecia nigrocincta (n = 6), Myrmecia tarsata (n = 16). Night-active: Myrmecia midas (n = 23), Myrmecia nigriceps (n = 10), and Myrmecia pyriformis (n = 18)

Species	Activity	Body mass (mg)	Brain mass (mg)	Optic lobes (mg)	Central brain (mg
M. croslandi	Day	26.059	0.551	0.18	0.371
M. croslandi	Day	15.219	0.515	0.164	0.351
M. croslandi	Day	23.594	0.564	0.19	0.374
M. croslandi	Day	14.298	0.44	0.162	0.278
M. croslandi	Day	17.16	0.52	0.186	0.334
M. croslandi	Day	20.997	0.533	0.17	0.363
M. croslandi	Day	24.925	0.561	0.19	0.371
M. gulosa	Day	24.624	0.845	0.202	0.643
M. gulosa	Day	73.623	1.213	0.34	0.873
M. gulosa	Day	23.351	0.85	0.18	0.67
M. gulosa	Day	70.207	1.174	0.332	0.842
M. gulosa	Day	110.076	1.292	0.394	0.898
M. gulosa	Day	98.83	1.365	0.428	0.937
M. gulosa	Day	19.895	0.788	0.148	0.64
M. gulosa	Day	29.103	0.844	0.18	0.664
M. gulosa	Day	55.055	0.975	0.284	0.691
M. gulosa	Day	68.202	1.104	0.338	0.766
M. gulosa	Day	41.244	1.022	0.274	0.748
M. gulosa	Day	109.074	1.267	0.396	0.871
-		26.048	0.874	0.24	0.634
M. gulosa	Day	89.034		0.356	0.808
M. gulosa	Day		1.164		
M. gulosa	Day	48.029	0.921	0.274	0.647
M. gulosa	Day	80.886	1.152	0.322	0.83
M. gulosa	Day	76.072	1.121	0.324	0.797
M. gulosa	Day	26.048	0.874	0.24	0.634
M. gulosa	Day	82.21	1.117	0.328	0.789
M. gulosa	Day	36.819	0.967	0.3	0.667
M. nigrocincta	Day	19.483	0.568	0.166	0.402
M. nigrocincta	Day	16.239	0.577	0.17	0.407
M. nigrocincta	Day	16.906	0.613	0.168	0.445
M. nigrocincta	Day	19.621	0.583	0.17	0.413
M. nigrocincta	Day	11.947	0.511	0.158	0.353
M. nigrocincta	Day	15.607	0.576	0.176	0.4
M. tarsata	Day	32.521	0.712	0.196	0.516
M. tarsata	Day	93.735	0.982	0.264	0.718
M. tarsata	Day	56.38	0.927	0.242	0.685
M. tarsata	Day	94.044	0.968	0.26	0.708
M. tarsata	Day	83.526	0.99	0.272	0.718
M. tarsata	Day	38.383	0.757	0.202	0.555
M. tarsata	Day	30.77	0.781	0.232	0.549
M. tarsata	Day	76.884	0.985	0.284	0.701
M. tarsata	Day	58.001	0.838	0.234	0.604
M. tarsata	Day	71.297	0.981	0.256	0.725
M. tarsata	Day	60.711	0.921	0.246	0.675
M. tarsata	Day	85.927	0.958	0.276	0.682
M. tarsata	Day	65.596	0.971	0.276	0.695
M. tarsata	Day	40.866	0.765	0.194	0.571
M. tarsata	Day	95.688	1.02	0.296	0.724
M. tarsata	Day	35.842	0.735	0.202	0.533

(Continues)

TABLE 2 (Continued)

Species	Activity	Body mass (mg)	Brain mass (mg)	Optic lobes (mg)	Central brain (mg)
M. midas	Night	53.375	1.033	0.214	0.819
M. midas	Night	176.98	1.588	0.31	1.278
M. midas	Night	173.55	1.687	0.378	1.309
M. midas	Night	56.575	1.251	0.22	1.031
M. midas	Night	106.208	1.394	0.332	1.062
M. midas	Night	72.338	1.125	0.244	0.881
M. midas	Night	41.98	0.91	0.194	0.716
M. midas	Night	97.124	1.4	0.308	1.092
M. midas	Night	147.656	1.573	0.4	1.173
M. midas	Night	41.681	1.149	0.21	0.939
M. midas	Night	24.273	0.865	0.14	0.725
M. midas	Night	22.167	0.839	0.12	0.719
M. midas	Night	57.414	1.44	0.3	1.14
M. midas	Night	66.934	1.28	0.26	1.02
M. midas	Night	100.186	1.4	0.316	1.084
M. midas	Night	83.857	1.268	0.26	1.008
M. midas	Night	105.375	1.384	0.32	1.064
M. midas	Night	72.835	1.182	0.236	0.946
M. midas	Night	33.988	0.876	0.124	0.752
M. midas	Night	46.325	0.904	0.15	0.754
M. midas	Night	70.17	1.101	0.242	0.859
M. midas	Night	89.125	1.22	0.278	0.942
M. midas	Night	87.207	1.284	0.24	1.044
	-		0.802	0.15	0.652
M. nigriceps M. nigriceps	Night Night	29.772 37.88	0.774	0.164	0.61
· ·	-		0.845	0.15	0.695
M. nigriceps	Night	40.513			
M. nigriceps	Night	51.948	0.85	0.17	0.68
M. nigriceps	Night	77.081	1.121	0.27	0.851
M. nigriceps	Night	74.33	1.125	0.246	0.879
M. nigriceps	Night	82.891	1.07	0.244	0.826
M. nigriceps	Night	99.754	1.232	0.286	0.946
M. nigriceps	Night	89.543	1.099	0.266	0.833
M. nigriceps	Night	83.681	1.113	0.218	0.895
M. pyriformis	Night	40.145	0.974	0.17	0.804
M. pyriformis	Night	49.047	1.061	0.24	0.821
M. pyriformis	Night	62.603	1.2	0.242	0.958
M. pyriformis	Night	77.132	1.237	0.27	0.967
M. pyriformis	Night	83.928	1.301	0.28	1.021
M. pyriformis	Night	94.456	1.35	0.324	1.026
M. pyriformis	Night	45.646	0.95	0.186	0.764
M. pyriformis	Night	22.306	0.607	0.106	0.501
M. pyriformis	Night	26.676	0.745	0.118	0.627
M. pyriformis	Night	119.796	1.471	0.352	1.119
M. pyriformis	Night	102.054	1.373	0.33	1.043
M. pyriformis	Night	127.825	1.509	0.384	1.125
M. pyriformis	Night	121.093	1.525	0.358	1.167
M. pyriformis	Night	27.773	0.782	0.154	0.628
M. pyriformis	Night	32.848	0.84	0.168	0.672
M. pyriformis	Night	52.452	1.082	0.258	0.824
M. pyriformis	Night	60.025	1.094	0.218	0.876
M. pyriformis	Night	72.051	1.225	0.31	0.915

1269

TABLE 3 Linear mixed effects model analyzing the allometric relationships between (a) brain weight and body weight, and (b) optic lobe weight and central brain weight

	Estimates	±SE	р
a. Full model (outcome: Brain weight)			
Intercept	-1.37325	0.15655	<.0001
Ln body weight	0.30684	0.03501	<.0001
Activity time	-0.19244	0.23260	.4443
Ln body weight \times activity time	0.09250	0.04874	.1114
a. Reduced model (outcome: Brain weight)			
Intercept	-1.57533	0.13759	<.0001
Ln body weight	0.35737	0.02902	<.0001
Activity time	0.20779	0.08701	.0723
b. Full model (outcome: Optic lobe weight)			
Intercept	-0.95357	0.09484	.0003
Ln central brain weight	1.02906	0.20772	.0052
Activity time	-0.29986	0.12422	.0969
Ln central brain weight \times activity time	0.52762	0.31147	.1625
b. Reduced model (outcome: Optic lobe weight)			
Intercept	-0.85563	0.07682	<.0001
Ln central brain weight	1.28297	0.16645	.0012
Activity time	-0.45950	0.07500	.0068

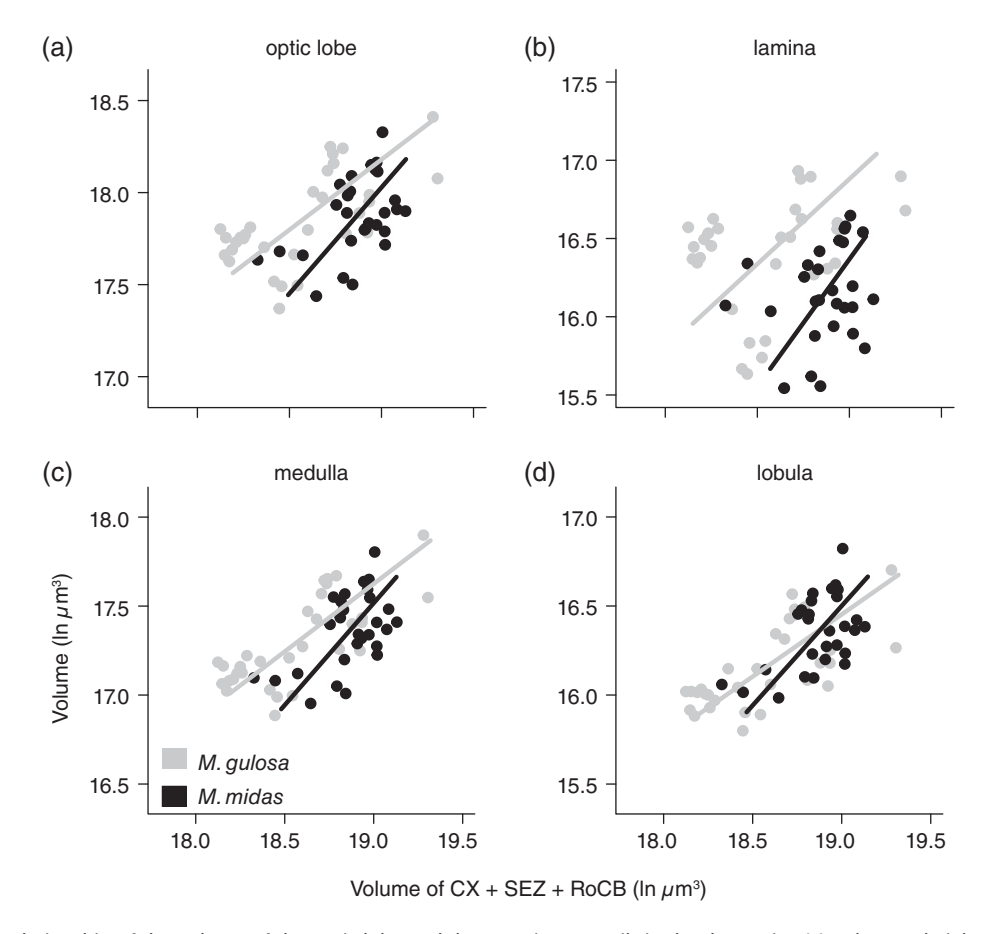


FIGURE 5 Scaling relationship of the volume of the optic lobe and three optic neuropils in the day-active *M. gulosa* and night-active *M. midas*. Scaling relations of the (a) entire optic lobe, (b) lamina, the first optic neuropil, (c) medulla, the second optic neuropil and (d) lobula, the third optic neuropil to the volume of CX + SEZ + RoCB for the day (gray) and night-active (black) ant species are shown. In each plot, regression lines are fitted to the data, which are outputs from standard major axis regression analysis (SMA). See Table 5 for statistical outputs

HW Species (mm) I	EB (μm³) OL (μm³)	n³) LA (μm³)	ME (μm³) 1	LO (μm³) A	AL (μm³)	C MB (µm³) LI	CA- LIP (µm³) (CA- COL (μm³)	PED + Lobes (µm³)	СХ (µm³)	CBU (µm³) C	CBL (µm³) N	NO (μm³) P	PB (µm³) SI	SEZ (μm³) F	RoCB (µm³)
M. gulosa 3.8	574,621,902.1 84,227,237.3 22,564,244	,237.3 22,564,244	46,000,507 15,662,487		15,859,057.3	90,260,006.2 43	43,299,110	13,764,994	33,195,902	2,353,079.4	1,334,298.8	429,920.98 15	158,716.3 4	430,143.28 3	34,467,867.5	98,388,322.9
M. gulosa 2.812	472,192,169.2 63,963,355.6 14,787,061	1,355.6 14,787,061	37,009,174 12,167,121		14,176,012.7	70,235,125.4 3:	31,436,272	12,516,607	26,282,247	2,153,885.22	1,184,876	407,485.43 14	143,345.36 4	418,178.41 3	34,543,370.6	92,766,889.8
M. gulosa 2.253	338,337,334.2 48,803,329.8	3,329.8 9,321,739	29,182,235 10,299,355		9,803,383.88	58,051,669.4 28	28,051,481	8,971,482.3	21,028,706	1,740,235.14	939,342.13	315,851.74 9	96,321.565 3	388,719.7 2.	22,759,480.4	69,895,838.3
M. gulosa 2.496	381,480,982.4 39,645,568.5 7,608,666.4 24,075,306 7,961,596.6 11,256,594.6	,568.5 7,608,666	4 24,075,306	7,961,596.6 1	11,256,594.6	63,938,418.5 2	29,359,171	8,993,394.6	25,585,853	2,211,798.28	1,201,243.8	494,689.57 11	116,507.6 3	399,357.29 2	24,548,844.6	86,365,848.4
M. gulosa 2.87	522,942,202.1 52,560,702.1 11,635,817	1,702.1 11,635,817		31,262,448 9,662,436.6 15,855	15,855,243.8	86,015,416.1 39	39,495,116	13,771,714	32,748,586	2,635,738.26 1	1,437,282.3	580,939.64 13	135,886.3 4	481,630.02 3	31,424,614.6 113,055,345	13,055,345
M. gulosa 3.134	594,991,790 76,996,669.5 16,606,875	,669.5 16,606,875		46,446,426 13,943,369 17,802,381.6	17,802,381.6	88,540,478.9 43,054,502		14,835,147	30,650,830	2,257,060.67 1	1,259,925.1	468,520.9 10	105,343.79 4	423,270.9 3:	32,340,220.9 1	103,077,373
M. gulosa 3.605	710,460,578.2 52,282,293.3 16,621,824	,293.3 16,621,824	27,381,878	8,278,590.9 10,673	10,673,427.4	61,200,566.1 30,386,064		10,539,153	20,275,350	1,308,498.64	725,135.02	261,793.59	63,345.725 2	258,224.3 2	20,660,697.9	63,217,551.3
M. gulosa 3.699	342,047,190.3 53,852,857.3 15,739,480	,857.3 15,739,480		29,053,222 9,060,155.4 11,482	11,482,582.8	58,161,033.5 28	28,552,014	8,161,681.1	21,447,338	1,284,365.76	830,052.54 208,217.11		125,122.94 120,973.17 20,613,605.4	20,973.17	0,613,605.4	52,498,427.1
M. gulosa 3.426	332,446,984.6 51,420,796.4 15,156,141	1,796.4 15,156,141	27,317,334	8,947,321.2 9,237	9,237,261.57	54,577,658.8 2	27,139,981	8,512,657.6	18,925,020	1,474,267.08	581,782.75 431,551.24		77,277.091 3	383,655.99 19,612,449	9,612,449	61,858,823.2
M. gulosa 3.478	335,930,846.3 50,167,689.8 14,573,913	7,689.8 14,573,913	26,416,711	9,177,065.2 10,607	10,607,500.4	53,671,724.8 20	26,942,571	9,075,544.1	17,653,610	1,420,826.45	755,788.97	316,148.15 9	97,260.203 251,629.13 20,975,129.3	51,629.13 2	0,975,129.3	58,727,649.8
M. gulosa 3.369	320,541,372.7 45,177,444.7 12,552,309	7,444.7 12,552,309	24,726,076 7,899,060		9,917,156.71	52,111,041.3 2	25,614,768	8,249,542.5	18,246,730	1,126,909.21	659,047.49	249,863.01	59,776.43 1	158,222.28 17,148,968.5	7,148,968.5	59,834,501.8
M. gulosa 3.516	721,696,924.6 70,880,807.1 17,516,038 41,778,663 11,586,107 18,451	,807.1 17,516,038	41,778,663	11,586,107 1	,344.9	110,471,560 5;	52,395,289	18,576,935	39,499,336	3,306,384.92	1,958,685.7	790,363.39 24	248,143.97 3	309,191.82 5	58,992,509.1	179,793,547
M. gulosa 2.078	360,860,735 34,970	34,970,618.8 6,163,863.1 21,536,002 7,270,753.4 10,889	.1 21,536,002	7,270,753.4 1	10,889,217.2	63,554,271.8 30	30,234,188	8,746,384.2	24,573,700	1,748,245.96	1,011,743.9	335,806.56	89,669.842 3	311,025.61 22,903,823.7	2,903,823.7	77,828,342.7
M. gulosa 2.079	565,427,072 62,542	62,542,391.5 15,562,036		36,347,498 10,632,858 16,085	16,085,508.3	94,983,941.7 4;	42,715,333	15,618,487	36,650,122	3,241,062.35 1	1,880,539	631,183.01 16	167,345.71 5	561,994.61 36,810,888.8		127,031,574
M. gulosa 3.769	344,339,111.9 51,203,551.1 13,971,950	1,551.1 13,971,950	28,339,437	8,892,163.8 9,498	9,498,474.69	57,936,575.5 28	28,965,410	9,674,197.6	19,296,968	1,163,553.15	566,468.13	205,364.15	83,192.982 3	308,527.89 20,725,822.1	0,725,822.1	62,452,264.8
M. gulosa 3.304	343,728,123.8 46,763,770.5 12,854,941	,770.5 12,854,941	25,743,237	8,165,593.3 9,827	9,827,874.15	51,585,844.6 25,457,463	5,457,463	8,311,404.4	17,816,978	1,333,574.05	680,905.97 238,293.55		81,021.293 333,353.24 19,290,179.8	33,353.24 1	9,290,179.8	55,517,960.7
M. gulosa 3.622	336,196,993.6 51,397,212	7,212 13,885,754	28,448,473	9,062,985.6 9,743	9,743,395.92	52,858,048.6 2	25,330,213	8,894,029.1	18,633,807	1,435,250.26	717,123.32 294,794.1		83,164.844 3	340,168 2	20,775,673.5	54,428,689.6
M. gulosa 2.35	343,486,320.4 54,376,947 15,605,378	,947 15,605,378	30,148,495	8,623,074.3 10,905	10,905,547.8	52,624,463.5 2	25,280,750	9,995,071.2	17,348,643	1,246,097.32	715,871.88	278,959.07	81,331.055 169,935.32		20,202,787.6	66,097,564.7
M. gulosa 3.52	589,360,423.8 81,051,054.8 21,453,036	,054.8 21,453,036	45,213,053 14,384,966	14,384,966 1	14,726,199.2	92,325,962.5 4	45,556,641	15,704,947	31,064,374	2,648,773.04 1	1,423,950.2	527,487.15 15	156,429.7 5	540,906.03 33,214,740.3		101,182,820
M. gulosa 3.383	590,506,636.1 73,981,853.7 17,636,344	,853.7 17,636,344		42,695,735 13,649,775 16,744,119	16,744,119	86,364,961 4:	41,657,626	14,514,977	30,192,358	2,064,090 1	1,087,177.6	409,950.21 12	125,518.15 4	441,443.99 34,959,763.3	4,959,763.3	96,119,881.5
M. gulosa 3.658	392,434,546.1 39,468,746.3 7,516,342.6 23,893,380	1,746.3 7,516,342.	.6 23,893,380	8,059,023.7 10,232	10,232,119.2	58,348,094.2 28	28,311,797	9,458,953.1	20,577,344	1,677,630.44	897,819.74	344,838.37 10	100,471.33 3	334,501 2	23,394,382.7	78,710,836.2
M. gulosa 3.617	342,689,416.4 48,151,766.7 12,951,255	,766.7 12,951,255		26,177,976 9,022,535.7 8,649	8,649,303.57	53,107,998.5 2	25,381,788	9,261,567.4	18,464,643	1,400,238.17	779,353.73	321,137.75 10	101,039.46	198,707.23 2	21,319,276	56,593,359.6
M. gulosa 3.222	523,515,645.5 65,945,385	3385 14,761,190	38,653,166 12,531,029		14,604,723.1	79,165,844.6 38	38,126,844	13,142,672	27,896,329	2,071,600.09 1	1,153,280.3	332,721.33 16	169,365.35 4	416,233.11 2	25,567,948.5	95,600,119.8
M. gulosa 3.018	649,947,161.4 64,880,176.1 16,189,018	0,176.1 16,189,018	37,249,499 11,441,659		15,379,821.4	95,556,331.9 43	43,666,747	14,641,548	37,248,037	3,158,814.4	1,809,578.8	649,235.92 20	201,320.38 4	498,679.3 3	37,178,501.7	126,975,420
M. gulosa 3.181	468,863,543.4 83,516,312.6 21,743,865	,312.6 21,743,865	47,223,581 14,548,867		17,060,118	96,159,549.6	46,688,684	16,913,291	32,557,575	2,485,169.25	1,228,676.3	446,849.96 16	163,740.08 6	645,902.89 4	41,236,108.5 1	100,969,109
M. gulosa 2.402	802,100,577.2 99,066,453.3 21,800,960	,453.3 21,800,960	59,326,544 17,938,949		20,907,062	114,292,385 5	55,222,274	20,773,022	38,297,089	3,157,736.43 1	1,897,253.8	624,863.87 16	166,193.39 4	469,425.4 5	59,099,723.8 1	173,793,238
M. gulosa 1.978	631,926,971.7 52,854,281.9 12,500,970	,281.9 12,500,970	31,005,321	9,347,991.2 22,132	22,132,207.1	91,314,999.2 3	37,942,374	13,646,667	39,725,958	3,254,667.09 1	1,851,012.5 7	754,319.51 17	174,606.52 4	474,728.52 3	39,381,118.7	122,639,276
M. gulosa 2.842	651,983,337.1 40,510,581.2		6,368,808.6 24,873,241	9,268,531.4 12,052,642.6	12,052,642.6	64,788,421.8 30	30,812,431	9,707,268.4	24,268,723	1,723,520.1	1,038,968.8	342,751.96 11	117,675.45 2	224,123.92 2	24,602,742.7	73,260,570.4
M. gulosa 2.72	490,017,188.1 53,600,857.4 12,450,094	1,857.4 12,450,094	31,718,740	9,432,023.4 10,670,277.5	10,670,277.5	75,687,764.9 3:	31,931,558	13,214,884	30,541,323	2,549,872.29 1	1,455,942.3	526,087.03 11	110,547.79 4	457,295.13 29,571,731.1	9,571,731.1	87,572,829
M. gulosa 3.131	756,263,254.7 46,909,041.2 6,842,685.8 29,765,032 10,301,323	,041.2 6,842,685.	.8 29,765,032		14,382,850.9	73,631,265.1 38	38,352,505	10,675,707	24,603,053	1,921,213.35 1	1,076,324	370,362.03 12	127,035.05 3	347,492.24 26,965,437.5	6,965,437.5	82,140,292.7
M. gulosa 3.858 1,108,758,613		58,749,542.9 12,077,591	36,032,533 10,639,418		19,696,564.7	97,736,293.2 4	45,973,701	15,964,351	35,798,241	2,761,150.7	1,666,772.8	521,347.99 14	143,947.36 4	429,082.57 3	35,506,376.9 120,052,337	20,052,337
M. midas 3.226	794,654,820 64,625	64,625,419.2 9,807,183.9 40,842,074 13,976,161	.9 40,842,074		19,352,211.7	108,257,482 5:	51,130,475	18,896,515	38,230,492	1,982,195.73 1	1,210,192.7	297,655.38 10	105,374 3	368,973.7	38,133,799.4 108,471,582	08,471,582
M. midas 3.146	960,805,901	58,797,656.4 7,860,372.4 37,308,342 13,628,942	.4 37,308,342		18,461,142.6	100,834,926 4	46,778,339	14,934,281	39,122,306	2,117,712.07	1,126,826.6	429,619.35 111,755.77		449,510.4 3	37,548,161.3 108,305,764	08,305,764
M. midas 3.226	M. midas 3.226 1,083,852,204 53,172,021.3 10,805,290 31,791,968 10,574,763 19,044,567.9	,021.3 10,805,290	31,791,968	10,574,763 1		111,815,721 5:	51,120,409	19,538,737	41,156,575	2,422,647.61 1,367,991.3		507,066.66 131,533.41		16,056.24 4	416,056.24 41,785,558.7 137,457,281	37,457,281
M. midas 2.191	783,224,610.9 37,414,760.5	.,760.5 5,629,536.	5,629,536.1 23,040,483 8,744,741.4 14,273	8,744,741.4 1	14,273,831.9	87,364,175.5 38,783,636		12,555,929	36,024,610	2,387,265.59 1,286,952.9		374,013.64 188,273.16		538,025.92 25,953,065.7		96,929,144.7

TABLE 4 (Continued)

HW Species (mm	HW (mm) EB (µm³)	OL (µm³)	LA (µm³)	ME (μm³) LO (μm³)	LO (µm³)	AL (µm³)	MB (μm³)	CA- LIP (μm³)	CA- COL (µm³)	PED + Lobes (μm^3)	CX (μm³) CBU (μm³)	CBL (μm³) NO (μm³)	n³) РВ (μm³)	, SEZ (μm³)	RoCB (µm³)
M. midas 3.8	M. midas 3.853 1,193,142,357		59,361,848.4 9,935,270.7 36,387,382 13,039,196	36,387,382		22,108,484.3	122,657,406	53,623,686	17,438,300	51,595,420	3,070,554.36 1,714,568.8	3 653,304.77 182,066.19		520,614.64 39,544,500.9 160,732,631	160,732,631
M. midas 3.6	3.646 408,560,878	408,560,878.2 45,583,974.5		9,549,559.4 26,606,481	9,427,934.5 12,013,384.	12,013,384.3	68,717,901.7 31,029,284		12,298,559	25,390,059	1,397,087.61 826,580.7	826,580.74 275,390.62 92,048.812 203,067.44 25,503,394.1	8.812 203,067	.44 25,503,394.1	64,160,116.3
M. midas 3.6	3.635 601,641,848	601,641,848.7 50,552,630.2		9,881,389.7 29,481,908 11,189,333	11,189,333	18,641,600.7	96,356,220.7 41,606,989	41,606,989	15,484,294	39,264,938	3,204,770.02 1,855,082.5	5 603,606.08 193,544.72		552,536.76 33,764,432.3 114,451,411	114,451,411
M. midas 3.7	3.798 749,117,818	749,117,818.6 54,010,535.9		8,364,187.8 33,970,336 11,676,012	11,676,012	19,811,000.9	110,032,714	47,981,407	17,415,625	44,635,682	3,147,167.36 1,694,198.7	7 506,881.8 241,019.45		705,067.39 34,648,020.5 126,082,687	126,082,687
M. midas 3.3	3.314 1,054,101,988	3 59,948,176.8		7,262,900.1 39,140,798 13,544,478	13,544,478	23,060,910.8	118,448,729	54,230,125	20,009,514	44,209,090	3,158,631.39 1,669,418.9	9 530,427.86 198,812.17	2.17 759,972.49	.49 27,999,499.6	27,999,499.6 162,948,619
M. midas 3.6	M. midas 3.699 1,011,386,807 39,851,701.2	7 39,851,701.2		5,702,205.4 24,368,272	9,781,223.5 17,945,684	17,945,684	97,331,063.2 44,108,252		15,666,946	37,555,865	2,639,392.71 1,382,257.5	5 522,875.16 105,442.95		628,817.09 34,502,049.3 115,396,260	115,396,260
M. midas 3.2	M. midas 3.217 689,232,662,7 55,080,998.3 9,415,073.2 33,900,677 11,765,248	2.7 55,080,998.3	9,415,073.2	33,900,677		21,913,688.7	125,206,780	59,385,374	19,714,975	46,106,431	2,619,729.77 1,585,398	434,360.37 128,811.34 471,160.07 39,000,483.4 132,148,764	1.34 471,160	.07 39,000,483.4	132,148,764
M. midas 3.584		449,004,554.1 47,701,976.9 12,481,864	12,481,864		26,197,199 9,022,914.8 13,395,343.	13,395,343.1	83,742,661.7 39,034,247		14,096,317	30,612,097	1,580,330.29 975,848.7	975,848.75 285,426.9 102,147.05		216,907.59 26,455,973.6	74,624,910.2
M. midas 2.867		601,170,707.5 61,412,920.7 11,463,983	7 11,463,983		35,942,480 14,006,457	18,053,790.9	116,823,843	55,774,694	18,807,493	42,241,656	2,580,056.92 1,241,040.2	2 472,184.39 174,500.24	0.24 692,332	692,332.09 39,773,803.7	97,355,228.1
M. midas 3.4	3.441 705,152,705	705,152,705.2 71,868,674.6 13,503,978	13,503,978	42,634,795 15,729,902	15,729,902	22,689,381.8	114,354,139	56,385,641	18,320,997	39,647,501	2,342,344.29 1,275,264.5	5 385,665.81 164,495.9		516,918.08 34,288,684.5 115,162,543	115,162,543
M. midas 3.5	3.517 898,439,999	898,439,999.4 68,576,508.3 12,362,111	12,362,111	41,893,866 14,320,531	14,320,531	22,037,618.3	118,371,509	58,033,700	16,947,803	43,390,006	2,287,140.07 1,164,022.5	5 456,721.56 162,804.32	4.32 503,591.72	72 37,584,553.7 102,573,933	102,573,933
M. midas 3.4	3.414 900,715,360	900,715,360.7 76,342,434.1 14,470,632	. 14,470,632	45,708,074 16,163,728	16,163,728	23,278,158.5	131,692,829	64,383,338	20,708,006	46,601,486	2,613,664.62 1,484,517.7	7 464,213.34 137,085.02		527,848.54 41,848,416.9 124,421,113	124,421,113
M. midas 3.6	M. midas 3.672 1,107,344,226 53,618,439.6 10,514,009	53,618,439.6	10,514,009	32,253,582 10,850,848	10,850,848	19,564,955.7	115,293,486	49,954,042	18,341,706	46,997,738	3,250,450.75 1,917,130.8	3 572,810.68 164,949.76	9.76 595,559.5		36,183,534.3 123,360,979
M. midas 4.236		780,292,690.8 74,480,048.2 14,301,363	: 14,301,363	43,688,789 16,489,896	16,489,896	22,422,287	130,445,237	67,227,488	19,672,621	43,545,128	2,691,853.67 1,662,686.3	3 343,739.17 145,772.98		539,655.19 41,221,640.7 128,592,315	128,592,315
M. midas 3.945		547,231,330 41,307,378.5 6,070,637.1 25,395,832 9,840,908.9 17,538,439.8	6,070,637.1	25,395,832	9,840,908.9	17,538,439.8	102,959,564	47,004,542	15,881,809	40,073,213	2,562,993.8 1,481,330.4	4 467,195.12 155,810.18 458,658.08 34,168,509.3 108,382,130	0.18 458,658	.08 34,168,509.3	108,382,130
M. midas 2.5	2.576 898,439,999	898,439,999.4 73,612,321.3 15,834,623	15,834,623	41,716,496 16,061,202	16,061,202	22,693,137.1	116,670,795	54,651,299	19,750,532	42,268,963	2,111,148.7 1,094,703.7	7 316,955.22 222,988.05		476,501.75 44,076,627.4 128,585,440	128,585,440
M. midas 2.7	2.727 677,195,988	677,195,988.8 55,629,797.1 9,660,974.5 33,225,594 12,743,228	9,660,974.5	33,225,594	12,743,228	19,999,782.1	121,509,736	56,042,598	19,565,694	45,901,443	2,534,681.57 1,425,808.7	7 492,942.52 172,512.53	2.53 443,417.8		37,184,151.8 126,940,554
M. midas 3.2	3.244 1,185,915,986	5 58,849,308.1	9,444,246.9	9,444,246.9 36,333,794 13,071,267	13,071,267	21,455,746.6	129,722,636	61,434,418	20,227,870	48,060,348	2,594,893.02 1,539,873.8	3 434,367.2 112,897.37		507,754.64 41,995,764.1 136,971,791	136,971,791
M. midas 3.7	3.752 635,317,161		66,108,680.3 12,034,675	38,990,485 15,083,520	15,083,520	17,358,927	106,863,830	52,281,873	19,762,433	34,819,523	2,298,576.63 1,358,147.7	7 381,321.75 132,928.45	8.45 426,178	426,178.77 40,127,756.7 108,207,021	108,207,021
M. midas 4.C	M. midas 4.017 1,000,785,467 77,294,900.5 15,593,250	77,294,900.5	15,593,250	46,250,852 15,450,799	15,450,799	17,366,436.1	123,204,162	61,594,004	21,227,302	40,382,856	2,594,222.95 1,353,590.3	3 460,093.25 171,128.56		609,410.82 46,122,813.9 125,122,417	125,122,417
M. midas 3.1	M. midas 3.143 851,518,423.8 91,144,562.9 16,962,403	3.8 91,144,562.9	16,962,403	53,959,150 20,223,010	20,223,010	25,093,455.5	132,277,221	63,437,519	22,080,871	46,758,831	2,478,943.55 1,447,441.9 493,056.78 144,204.47 394,240.41 43,286,055.2 133,731,468	9 493,056.78 144,20	4.47 394,240	.41 43,286,055.2	133,731,468
M. midas 3.3	3.394 524,064,159	524,064,159.2 46,702,460		9,203,050.7 27,253,902 10,245,507	10,245,507	17,468,130.1	83,162,698.1 40,840,517		13,913,853	28,408,328	2,154,804.44 1,193,070.8	3 332,030.9 135,324.45 494,378.25 25,951,084.8	4.45 494,378	.25 25,951,084.8	88,333,927.4
M. midas 4.338		741,743,530.4 62,980,122.1 15,258,395	15,258,395	34,934,240 12,787,487	12,787,487	23,868,062.5	112,819,778	51,008,696	16,621,074	45,190,007	3,862,890.55 2,278,322.7	7 580,369.68 249,816.69 754,381.46 41,226,245.7 147,037,750	6.69 754,381	.46 41,226,245.7	147,037,750
M. midas 3.818		718,643,422.6 49,453,386.2 7,973,953.4 30,247,491 11,231,942	7,973,953.4	1 30,247,491	11,231,942	20,848,166.1	128,596,292	56,057,842	19,869,512	52,668,938	3,222,554.74 1,757,278.8	3 559,712.4 173,722.16 731,841.35 42,397,791.4 136,472,776	2.16 731,841	.35 42,397,791.4	136,472,776

HW = head width; EB = entire brain; OL = optic lobe; LA = lamina; ME = medulla; LO = lobula; AL = antennal lobe; MB = mushroom body; CA-LIP = calyx lip; CA-COL = calyx collar; PED+Lobes = peduncle and lobes; CX = central complex; CBU = central body upper unit; CBL = central body lower unit; NO = nodull; PB = protocerebral bridge; SEZ = subesophageal zone; RoCB = rest of the central brain.

TABLE 5 Outputs of standardized major axis regression (SMA) on log transformed data (log $y = \alpha + \beta \cdot \log x$) determining the scaling relationships of each neuropil volume with the volume of the reference structure in the day-active *M. gulosa* and night-active *M. midas*

у	x (reference structure)	Do groups have common slope?	Scaling slope, β [95% CI]	Is β different from 1?	Grade shift?	$\alpha_{ ext{gulosa}}$	α_{midas}	gsi
OL	CX + SEZ + RoCB	Yes $\chi^2 = 3.267$ $p = .071$	0.902 [0.718, 1.137]	No $\chi^2 = 4.053$ $p = .132$	Yes $W^2 = 14.21$ $p = 1.64 \times 10^{-4}$	1.095	0.849	1.278
LA	CX + SEZ + RoCB	Yes $\chi^2 = 2.343$ $p = .126$	1.308 [1.003, 1.704]	Yes $\chi^2 = 6.269$ $p = .044$	Yes $W^2 = 29.66$ $p = 5.15 \times 10^{-8}$	-7.872	-8.524	1.919
ME	CX + SEZ + RoCB	Yes $\chi^2 = 3.738$ $p = .053$	0.881 [0.716, 1.089]	No $\chi^2 = 5.143$ $p = .076$	Yes $W^2 = 11.61$ $p = 1.65 \times 10^{-4}$	0.936	0.740	1.216
LO	CX + SEZ + RoCB	No $\chi^2 = 5.416$ $p = .019$	n/a	n/a	n/a	n/a	n/a	n/a
AL	CX + SEZ + RoCB	Yes $\chi^2 = 0.783$ $p = .376$	0.870 [0.761, 0.996]	No $\chi^2 = 4.865$ $p = .088$	Yes $W^2 = 15.23$ $p = 9.50 \times 10^{-5}$	0.230	0.366	0.872
МВ	CX + SEZ + RoCB	Yes $\chi^2 = 0.698$ $p = .404$	0.791 [0.716, 0.875]	Yes $\chi^2 = 17.95$ $p = .0001$	Yes $W^2 = 46.4$ $p = 9.62 \times 10^{-12}$	3.412	3.591	0.836
CA-LIP	CX + SEZ + RoCB	Yes $\chi^2 = 2.982$ $p = .084$	0.785 [0.690, 0.899]	Yes $\chi^2 = 14.09$ $p = .001$	Yes $W^2 = 25.84$ $p = 3.72 \times 10^{-7}$	2.771	2.935	0.848
CA-COL	CX + SEZ + RoCB	Yes $\chi^2 = 0.001$ $p = .974$	0.839 [0.743, 0.947]	Yes $\chi^2 = 7.758$ $p = .021$	Yes $W^2 = 26.08$ $p = 3.28 \times 10^{-7}$	0.702	0.863	0.851
PED+Lobes	CX + SEZ + RoCB	Yes $\chi^2 = 0.222$ $p = .638$	0.881 [0.786, 0.993]	Yes $\chi^2 = 7.53$ $p = .023$	Yes $W^2 = 57.03$ $p = 4.28 \times 10^{-14}$	0.714	0.881	0.846
CX	SEZ + RoCB	Yes $\chi^2 = 0.486$ $p = .486$	1.061 [0.946, 1.192]	No $\chi^2 = 1.534$ $p = .464$	No $W^2 = 3.49$ $p = .062$	-5.186	-5.260	1.076
CBU	SEZ + RoCB	Yes $\chi^2 = 0.006$ $p = .939$	1.145 [1.013, 1.294]	No $\chi^2 = 4.641$ $p = .098$	No $W^2 = 3.25$ $p = .071$	-7.335	-7.416	1.084
CBL	SEZ + RoCB	Yes $\chi^2 = 0.435$ $p = .509$	1.148 [0.989, 1.336]	No $\chi^2 = 3.744$ $p = .154$	Yes $W^2 = 20.14$ $p = 7.19 \times 10^{-6}$	-8.404	-8.648	1.276
NO	SEZ + RoCB	Yes $\chi^2 = 2.096$ $p = .148$	1.124 [0.945, 1.344]	No $\chi^2 = 3.843$ $p = .146$	No $W^2 = 1.73$ $p = .188$	-9.161	-9.248	1.090
РВ	SEZ + RoCB	Yes $\chi^2 = 2.516$ $p = .113$	1.395 [1.127, 1.724]	Yes $\chi^2 = 11.66$ $p = .003$	No $W^2 = 0.55$ $p = .459$	-13.107	-13.174	1.069
SEZ	CX + RoCB	Yes $\chi^2 = 0.671$ $p = .413$	0.945 [0.843 1.056]	No $\chi^2 = 1.695$ $p = .429$	No $W^2 = 0.51$ $p = .476$	-0.132	-0.160	1.028

Abbreviations of brain structures as described in Table 4.

gsi values >1 indicates that the structure is larger in diurnal ants, and gsi <1 indicates that the structure is larger in nocturnal ants.

sensory capabilities. Relative to body mass, brain size did not differ between nocturnal and diurnal species. But night-active ants had relatively smaller optic lobes, larger antennal lobes, and larger mushroom bodies compared to congeneric day-active species.

Though several nocturnal ants have evolved distinct visual adaptations for low light environments (Greiner et al., 2007; Narendra et al., 2017), their brain organization and investment into different neuropil has not been studied previously. We found that the day-active *Myrmecia* ants invested more into their optic lobes compared to their night-active relatives (Figure 4b). Interestingly, among the day-active species, the ant with the smallest brain, *M. croslandi*, made the largest investment into their optic lobes relative to the size of the central brain (Figure 4). The

only distinct visually guided behavior we know that sets *M. croslandi* apart is their ability to visually track flying insects and jump to capture them. It remains to be identified whether this hunting behavior has led to a significantly higher investment in their optic lobes.

4.1 | Peripheral and higher order sensory neuropils: Vision

Accessing visual information in dim-light conditions is difficult due to low visual signal-to-noise ratio. Thus, nocturnal ants have evolved distinct visual adaptations to improve optical sensitivity (Greiner et al., 2007; Narendra et al., 2011; Narendra, Greiner, Ribi, & Zeil, 2016;

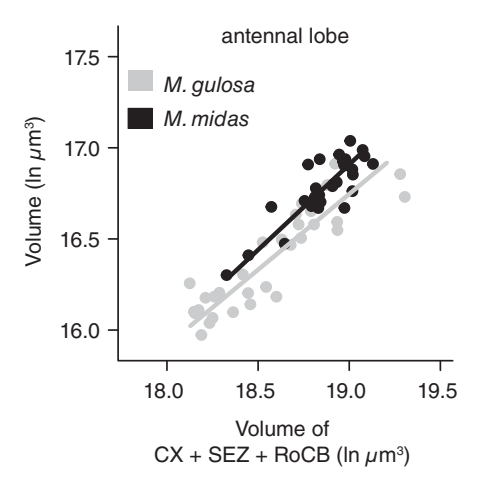


FIGURE 6 Scaling relationship of the volume of the antennal lobe in the day-active *M. gulosa* and night-active *M. midas*. Conventions as described in Figure 5

Narendra & Ribi, 2017). It is evident from our results that dim-light conditions have driven changes in sensory neuropils as well. From both weight and volumetric measurements, we found that visually oriented nocturnal ants tend to have smaller optic lobes compared to their diurnal relatives (Figures 4b and 5a). Volumetric estimates were less than the weight measurements because weight measurements included cell bodies and axon connections between the optic lobe

neuropils, which the volume measurements did not. In addition, for volumetric estimates, samples were dehydrated and cleared in methyl salicylate, both of which lead to tissue shrinkage. Although the optic lobes were smaller in nocturnal ants, the visual input region of the mushroom bodies, the calyx collar, was significantly larger compared to the diurnal ants (Figure 7c). Our findings in the visually mediated ants were different to those found in the nocturnal hawkmoths, which rely less on vision. The nocturnal hawkmoths had smaller optic lobes and smaller visual input regions in the mushroom body compared to their diurnal counterparts (Stöckl, Heinze, et al., 2016). While the visual circuitry in nocturnal ants needs to be analyzed, perhaps small optic lobes are sufficient for nocturnal *Myrmecia*, if they are similar to the nocturnal bees and engage in spatial summation (Greiner et al., 2004).

The increase in the size of the mushroom body calyx collar in nocturnal ants most likely allows for an increase in visual information processing capacity (Ehmer & Gronenberg, 2004; Niven & Laughlin, 2008), which may allow animals to be active in dim-light conditions. It is unknown how this increase in size of the mushroom body calyx collar reflects the number of Kenyon cells and afferent sensory neurons innervating this region and the number of synaptic clusters contained within. There is thus a need to investigate the information processing capacities of nocturnal animals at the level of individual neurons.

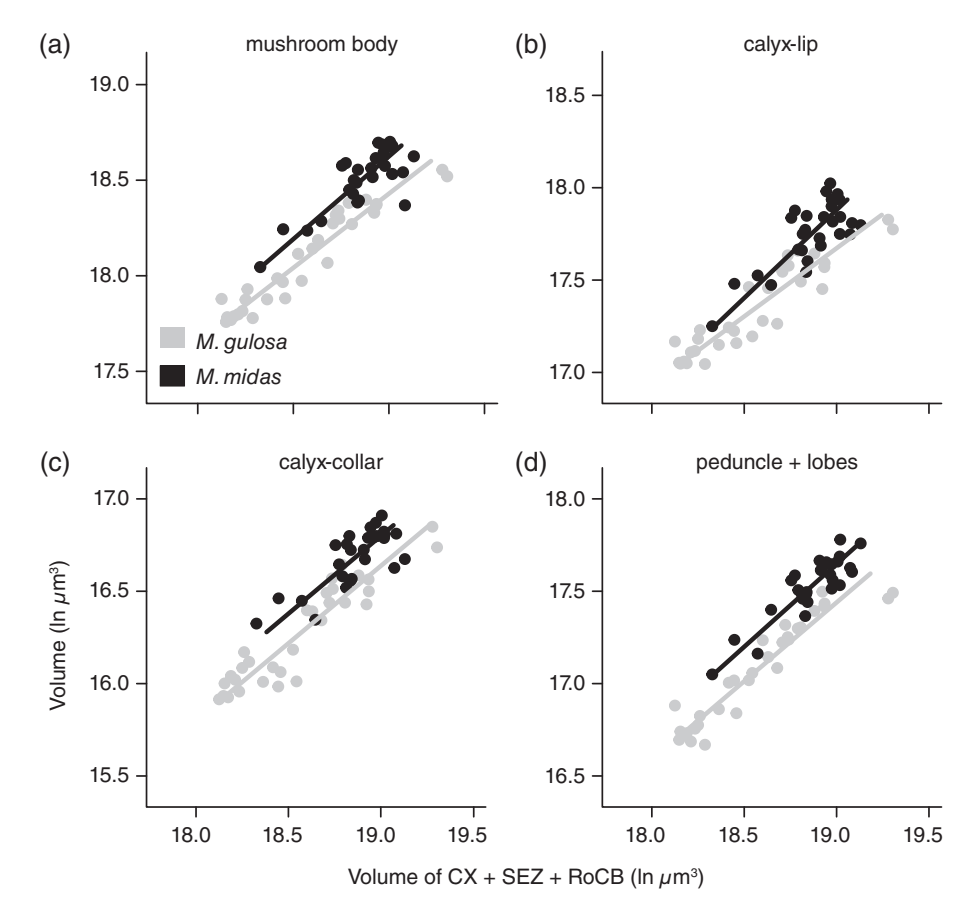


FIGURE 7 Scaling relationship of the volume of the mushroom body and its subregions in the day-active *M. gulosa* and night-active *M. midas*. Scaling relationship is shown for (a) entire mushroom body, (b) mushroom body calyx-lip region, (c) mushroom body calyx-collar region and (d) peduncle + lobes. Conventions as described in Figure 5

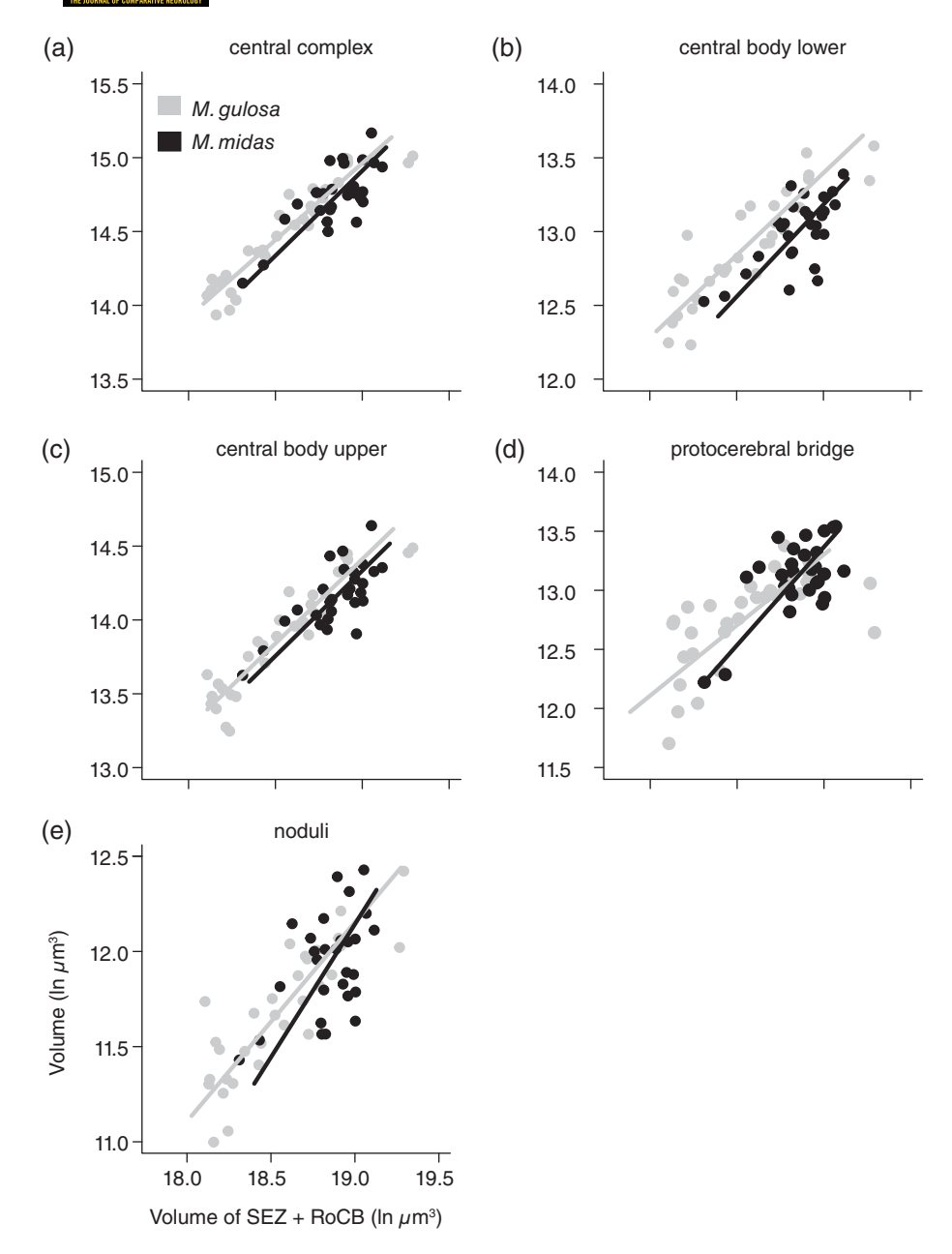


FIGURE 8 Scaling relationship of the volume of the central complex and its subregions in the day-active *M. gulosa* and night-active *M. midas*. Scaling relationship of (a) entire central complex, (b) central body upper unit, (c) central body lower unit, (d) noduli, and (e) protocerebral bridge with volume of SEZ + RoCB is shown. Conventions as described in Figure 5

4.2 | Peripheral and higher order sensory neuropils: Olfaction

Ants, irrespective of whether they are day- or night-active, require the ability to detect and process odor information for social interactions within the dark confines of the nest where vision is unlikely to play a significant role. Therefore, it is unclear why the investment pattern in the antennal lobes and olfactory input region in the mushroom body calyx (CA-Lip) differs. Both nocturnal ants and hawkmoths (Stöckl, Heinze, et al., 2016) invested more in the antennal lobes and olfactory input region in the mushroom body calyx (Figures 6 and 7b). In the nocturnal *Myrmecia*, there is strong behavioral data supporting the use of visual information for navigating in dim-light conditions (Freas

et al., 2018; Narendra & Ramirez-Esquivel, 2017; Reid et al., 2011). Nonetheless, the greater investment that nocturnal ants appear to make toward detecting and processing odor information may be required for carrying out tasks outside the nest. The nocturnal *Myrmecia* ants are solitary foragers and despite having no recruitment strategy all foragers from a single nest "agree" to forage on specific trees and remain faithful to these trees for the entire life of the nest. While animals use visual information to revisit the same tree over their entire lifetime, odor information associated with the tree may allow ants to converge on the same tree during their first foraging trip. In addition, once ants have reached the tree, odor information could allow them to orient toward specific food resources (e.g., sap, aphids, insect prey) in low light conditions.

4.3 | Multisensory integration center

The central complex is a highly conserved region that has been identified to be vital for processing spatial information, controlling locomotion and orientation, and integrating multisensory information (Heinze, 2017; Heinze et al., 2018; Pfeiffer & Homberg, 2014; Seelig & Jayaraman, 2015; Stone et al., 2017; Strauss & Heisenberg, 1993). It is perhaps because the function of the central complex is integral to the performance of many fundamental behaviors that its size did not vary between the diurnal and nocturnal species (Figure 8). However, the central body lower unit was significantly smaller in the nocturnal species (Figure 8b). The central body lower unit relays celestial compass information into the central complex and in Drosophila the ring neurons in the ellipsoid body (homologous to the central body lower unit) encode landmark information (Seelig & Jayaraman, 2015), all of which confirm this region's important role in navigation. It is unknown how or whether the reduced size of the central body lower unit affects orientation in any arthropod. In addition, documentation of the extent of the dorsal rim area, which detects celestial compass information (Meyer & Labhart, 1993; Narendra, Ramirez-Esquivel, & Ribi, 2016; Zeil, Ribi, & Narendra, 2014), in the dayand night-active species along with a robust behavioral paradigm to test orientation precision in day- and night-active animals is required to fully assess the ecological significance of this volume difference.

In summary, there are clear differences in the size of functionally distinct brain regions between closely related diurnal and nocturnal *Myrmecia* ants. Despite being visually mediated, the nocturnal ants invested less in their optic lobes yet more in the higher-order visual processing regions. The ecological relevance of these size differences, particularly why the nocturnal ants have smaller optic lobes, remains to be identified. However, the size of the primary and higher-order sensory brain regions appears to be adapted to the ants' temporal niche. These neural adaptations, in addition to the optical adaptions, may be the key to enabling ants to access and process visual information in dim-light environments.

ACKNOWLEDGMENTS

We are grateful to Wulfila Gronenberg and Stanley Heinze for their comments on an earlier version and Debjani Das for statistical advice. We thank Sue Lindsay for providing us access to the confocal microscope at Macquarie University. We are grateful to two anonymous reviewers for their comments. The study was supported by grants from the Australian Research Council (FT140100221, DP150101172) and from the Macquarie University Species Spectrum Research Centre.

CONFLICT OF INTEREST

The authors have no conflicting interests.

AUTHORS CONTRIBUTIONS

Volumetric data: ZS, JFK; weights data: MAS, AN; Data analyses: ZS, JFK, MAS, AN; First draft: ZS; Revision: ZS, JFK, MAS, AN. Conceived and designed the study: JFK, AN. All authors gave final approval for publication.

ORCID

Ajay Narendra https://orcid.org/0000-0002-1286-5373

REFERENCES

- Bressan, J. M. A., Benz, M., Oettler, J., Heinze, J., Hartenstein, V., & Sprecher, S. G. (2015). A map of brain neuropils and fiber systems in the ant *Cardiocondyla obscurior*. Frontiers in Neuroanatomy, 8, 363. http://doi.org/10.3389/fnana.2014.00166
- Bucher, D., Scholz, M., Stetter, M., Obermayer, K., & Pflüger, H.-J. (2000). Correction methods for three-dimensional reconstructions from confocal images: I. Tissue shrinking and axial scaling. *Journal of Neuroscience Methods*, 100(1–2), 135–143. http://doi.org/10.1016/S0165-0270(00) 00245-4
- Bulova, S., Purce, K., Khodak, P., Sulger, E., & O'Donnell, S. (2016). Into the black and back: The ecology of brain investment in Neotropical army ants (Formicidae: Dorylinae). Science of Nature, 103(3-4), 31. http:// doi.org/10.1007/s00114-016-1353-4
- Collett, T. S., & Zeil, J. (2018). Insect learning flights and walks. Current Biology, 28(17), R984–R988. http://doi.org/10.1016/j.cub.2018. 04.050
- Cronin, T. W., Johnsen, S., Marshall, J., & Warrant, E. J. (2014). Visual ecology (pp. 1–428). Princeton and Oxford, England: Princeton University Press.
- Ehmer, B., & Gronenberg, W. (2004). Mushroom body volumes and visual interneurons in ants: Comparison between sexes and castes. *The Journal of Comparative Neurology*, 469(2), 198–213. http://doi.org/10. 1002/cne.11014
- El Jundi, B., Huetteroth, W., Kurylas, A. E., & Schachtner, J. (2009). Anisometric brain dimorphism revisited: Implementation of a volumetric 3D standard brain in *Manduca sexta*. The Journal of Comparative Neurology, 517(2), 210–225. http://doi.org/10.1002/cne.22150
- Eriksson, E. S. (1985). Attack behaviour and distance perception in the Australian bulldog ant Myrmecia nigriceps. Journal of Experimental Biology, 119(1), 115–131.
- Freas, C. A., Narendra, A., & Cheng, K. (2017). Compass cues used by a nocturnal bull ant, *Myrmecia midas. Journal of Experimental Biology*, 220, 1578–1585. http://doi.org/10.1242/jeb.152967
- Freas, C. A., Narendra, A., Lemesle, C., & Cheng, K. (2017). Polarized light use in the nocturnal bull ant, *Myrmecia midas. Royal Society Open Science*, 4(8), 170598–170511. http://doi.org/10.1098/rsos.170598
- Freas, C. A., Wystrach, A., Narendra, A., & Cheng, K. (2018). The view from the trees: Nocturnal bull ants, *Myrmecia midas*, use the surrounding panorama while descending from trees. *Frontiers in Psychology*, *9*, 16. http://doi.org/10.3389/fpsyg.2018.00016
- Greiner, B. (2006). Adaptations for nocturnal vision in insect apposition eyes. *International Review of Cytology*, 250, 1–46.
- Greiner, B., Narendra, A., Reid, S. F., Dacke, M., Ribi, W. A., & Zeil, J. (2007). Eye structure correlates with distinct foraging-bout timing in primitive ants. *Current Biology*, 17(20), R879–R880. http://doi.org/10.1016/j.cub.2007.08.015
- Greiner, B., Ribi, W. A., & Warrant, E. J. (2005). A neural network to improve dim-light vision? Dendritic fields of first-order interneurons in the nocturnal bee *Megalopta genalis*. *Cell and Tissue Research*, 322(2), 313–320. http://doi.org/10.1007/s00441-005-0034-y
- Greiner, B., Ribi, W. A., Wcislo, W. T., & Warrant, E. J. (2004). Neural organisation in the first optic ganglion of the nocturnal bee *Megalopta genalis*. *Cell and Tissue Research*, *318*(2), 429–437. http://doi.org/10.1007/s00441-004-0945-z
- Groh, C., Lu, Z., Meinertzhagen, I. A., & Rössler, W. (2012). Age-related plasticity in the synaptic ultrastructure of neurons in the mushroom body calyx of the adult honeybee Apis mellifera. The Journal of Comparative Neurology, 520(15), 3509–3527. http://doi.org/10.1002/cne. 23102
- Gronenberg, W., Heeren, S., & Hölldobler, B. (1996). Age-dependent and task-related morphological changes in the brain and the mushroom bodies of the ant *Camponotus floridanus*. *Journal of Experimental Biology*, 199, 2011–2019.

- Hasegawa, E., & Crozier, R. (2006). Phylogenetic relationships among species groups of the ant genus Myrmecia. Molecular Phylogenetics and Evolution, 38, 575–582.
- Heinze, S. (2017). Unraveling the neural basis of insect navigation. *Current Opinion in Insect Science*, 24, 58–67. http://doi.org/10.1016/j.cois. 2017.09.001
- Heinze, S., Narendra, A., & Cheung, A. (2018). Principles of insect path integration. *Current Biology*, 28(17), R1043–R1058. http://doi.org/10.1016/j.cub.2018.04.058
- Heinze, S., & Reppert, S. M. (2012). Anatomical basis of sun compass navigation I: The general layout of the monarch butterfly brain. *The Journal of Comparative Neurology*, 520(8), 1599–1628. http://doi.org/10.1002/cne.23054
- Hell, S., Reiner, G., Cremer, C., & Stelzer, E. H. K. (1993). Aberrations in confocal fluorescence microscopy induced by mismatches in refractive index. *Journal of Microscopy*, 169(3), 391–405. http://doi.org/10.1111/ j.1365-2818.1993.tb03315.x
- Kamhi, J. F., Gronenberg, W., Robson, S. K. A., & Traniello, J. F. A. (2016). Social complexity influences brain investment and neural operation costs in ants. *Proceedings of the Royal Society B*, 283(1841), 20161949. http://doi.org/10.1098/rspb.2016.1949
- Kamhi, J. F., Sandridge-Gresko, A., Walker, C., Robson, S. K. A., & Traniello, J. F. A. (2017). Worker brain development and colony organization in ants: Does division of labor influence neuroplasticity? *Developmental Neurobiology*, 77(9), 1072–1085. http://doi.org/10.1002/dneu.22496
- Land, M., & Fernald, R. (1992). The evolution of eyes. *Annual Review of Neuroscience*, 15, 1–29.
- Land, M. F., & Nilsson, D.-E. (2012). Animal eyes. Oxford, England: Oxford University Press.
- Meyer, E. P., & Labhart, T. (1993). Morphological specializations of dorsal rim ommatidia in the compound eye of dragonflies and damselfies (Odonata). Cell and Tissue Research, 272(1), 17–22. http://doi.org/10. 1007/BF00323566
- Montgomery, S. H., & Ott, S. R. (2015). Brain composition in *Godyris zavaleta*, a diurnal butterfly, reflects an increased reliance on olfactory information. *The Journal of Comparative Neurology*, 523(6), 869–891. http://doi.org/10.1002/cne.23711
- Muscedere, M. L., Gronenberg, W., Moreau, C. S., & Traniello, J. F. A. (2014). Investment in higher order central processing regions is not constrained by brain size in social insects. *Proceedings of the Royal Society B*, 281(1784), 20140217. http://doi.org/10.1098/rspb.2014.0217
- Muscedere, M. L., & Traniello, J. F. A. (2012). Division of labor in the hyperdiverse ant genus *Pheidole* is associated with distinct subcaste-and age-related patterns of worker brain organization. *PLoS One*, 7(2), e31618. http://doi.org/10.1371/journal.pone.0031618
- Narendra, A., Gourmaud, S., & Zeil, J. (2013). Mapping the navigational knowledge of individually foraging ants, Myrmecia croslandi. Proceedings of the Royal Society B, 280(1765), 20130683. http://doi.org/10. 1242/ieb.02768
- Narendra, A., Greiner, B., Ribi, W. A., & Zeil, J. (2016). Light and dark adaptation mechanisms in the compound eyes of *Myrmecia* ants that occupy discrete temporal niches. *Journal of Experimental Biology*, 219, 2435–2442.
- Narendra, A., Kamhi, J. F., & Ogawa, Y. (2017). Moving in dim light: Behavioral and visual adaptations in nocturnal ants. *Integrative and Comparative Biology*, 57, 1104–1116. http://doi.org/10.1093/icb/icx096
- Narendra, A., & Ramirez-Esquivel, F. (2017). Subtle changes in the landmark panorama disrupt visual navigation in a nocturnal bull ant. *Philo-sophical Transactions of the Royal Society B*, 372, 20160068.
- Narendra, A., Ramirez-Esquivel, F., & Ribi, W. A. (2016). Compound eye and ocellar structure for walking and flying modes of locomotion in the Australian ant, *Camponotus consobrinus*. *Scientific Reports*, 6(1), 22331. http://doi.org/10.1038/srep22331
- Narendra, A., Reid, S. F., Greiner, B., Peters, R. A., Hemmi, J. M., Ribi, W. A., & Zeil, J. (2011). Caste-specific visual adaptations to distinct daily activity schedules in Australian Myrmecia ants. Proceedings of the Royal Society B, 278(1709), 1141–1149. http://doi.org/10.1098/ rspb.2010.1378
- Narendra, A., Reid, S. F., & Hemmi, J. M. (2010). The twilight zone: Ambient light levels trigger activity in primitive ants. *Proceedings of the Royal Society B*, 277, 1531–1538.

- Narendra, A., Reid, S. F., & Raderschall, C. A. (2013). Navigational efficiency of nocturnal *Myrmecia* ants suffers at low light levels. *PLoS One*, 8(3), e58801. http://doi.org/10.1371/journal.pone.0058801.g004
- Narendra, A., & Ribi, W. A. (2017). Ocellar structure is driven by the mode of locomotion and activity time in *Myrmecia* ants. *Journal of Experimental Biology*, 220(23), 4383–4390. http://doi.org/10.1242/jeb. 159392
- Niven, J. E., & Laughlin, S. B. (2008). Energy limitation as a selective pressure on the evolution of sensory systems. *Journal of Experimental Biology*, 211(11), 1792–1804. http://doi.org/10.1242/jeb.017574
- O'Carroll, D. C., & Warrant, E. J. (2017). Vision in dim light: Highlights and challenges. *Philosophical Transactions of the Royal Society B*, 372(1717), 20160062. http://doi.org/10.1098/rstb.2016.0062
- O'Donnell, S., & Bulova, S. (2017). Development and evolution of brain allometry in wasps (Vespidae): Size, ecology and sociality. *Current Opinion in Insect Science*, 22, 54–61. http://doi.org/10.1016/j.cois.2017. 05.014
- O'Donnell, S., Clifford, M. R., DeLeon, S., Papa, C., Zahedi, N., & Bulova, S. J. (2013). Brain size and visual environment predict species differences in paper wasp sensory processing brain regions (hymenoptera: Vespidae, Polistinae). *Brain, Behavior and Evolution, 82*(3), 177–184. http://doi.org/10.1159/000354968
- Ogata, K. (1991). Ants of the genus *Myrmecia* Fabricius: A review of the species groups and their phylogenetic relationships (Hymenoptera: Formicidae: Myrmeciinae). *Systematic Entomology*, *16*, 353–381.
- Ogata, K., & Taylor, R. W. (1991). Ants of the genus *Myrmecia* Fabricius: A preliminary review and key to the named species (Hymenoptera: Formicidae: Myrmeciinae). *Journal of Natural History*, 25, 1623–1673.
- Ott, S. R., & Rogers, S. M. (2010). Gregarious desert locusts have substantially larger brains with altered proportions compared with the solitarious phase. *Proceedings of the Royal Society B*, 277(1697), 3087–3096. http://doi.org/10.1098/rspb.2010.0694
- Pfeiffer, K., & Homberg, U. (2014). Organization and functional roles of the central complex in the insect brain. *Annual Review of Entomology*, *59*(1), 165–184. http://doi.org/10.1146/annurev-ento-011613-162031
- Reid, S. F., Narendra, A., Hemmi, J. M., & Zeil, J. (2011). Polarised skylight and the landmark panorama provide night-active bull ants with compass information during route following. *Journal of Experimental Biology*, 214, 363–370.
- Ribi, W. A. (1975). Golgi studies in the first optic ganglion of the ant Cataglyhis bicolor. Cell and Tissue Research, 160, 207–217.
- Schindelin, J., Arganda-Carreras, I., Frise, E., Kaynig, V., Longair, M., Pietzsch, T., ... Cardona, A. (2012). Fiji: An open-source platform for biological-image analysis. *Nature Methods*, 9(7), 676–682. http://doi. org/10.1038/nmeth.2019
- Seelig, J. D., & Jayaraman, V. (2015). Neural dynamics for landmark orientation and angular path integration. *Nature*, 521(7551), 186–191. http://doi.org/10.1038/nature14446
- Seid, M. A., Castillo, A., & Wcislo, W. T. (2011). The allometry of brain miniaturization in ants. *Brain, Behavior and Evolution, 77*(1), 5–13. http://doi.org/10.1159/000322530
- Somanathan, H., Kelber, A., Borges, R. M., Wallen, R., & Warrant, E. J. (2009). Visual ecology of Indian carpenter bees II: Adaptations of eyes and ocelli to nocturnal and diurnal lifestyles. *Journal of Comparative Physiology* A, 195, 571–583.
- Stieb, S. M., Muenz, T. S., Wehner, R., & Rössler, W. (2010). Visual experience and age affect synaptic organization in the mushroom bodies of the desert ant *Cataglyphis fortis*. *Developmental Neurobiology*, 70(6), 408–423. http://doi.org/10.1002/dneu.20785
- Stöckl, A., Heinze, S., Charalabidis, A., El Jundi, B., Warrant, E. J., & Kelber, A. (2016). Differential investment in visual and olfactory brain areas reflects behavioural choices in hawk moths. *Scientific Reports*, 6, 26041. http://doi.org/10.1038/srep26041
- Stöckl, A. L., O'Carroll, D. C., & Warrant, E. J. (2016). Neural summation in the hawkmoth visual system extends the limits of vision in dim light. *Current Biology*, 26(6), 821–826. http://doi.org/10.1016/j.cub.2016. 01.030
- Stöckl, A. L., Ribi, W. A., & Warrant, E. J. (2016). Adaptations for nocturnal and diurnal vision in the hawkmoth lamina. *The Journal of Comparative Neurology*, 524(1), 160–175. http://doi.org/10.1002/cne. 23832

1277

- Stone, T., Webb, B., Adden, A., Weddig, N. B., Honkanen, A., Templin, R., et al. (2017). An anatomically constrained model for path integration in the bee brain. *Current Biology*, *27*(20), 3069–3085.e11. http://doi.org/10.1016/j.cub.2017.08.052
- Strauss, R., & Heisenberg, M. (1993). A higher control center of locomotor behavior in the *Drosophila* brain. *Journal of Neuroscience*, 13(5), 1852–1861. http://doi.org/10.1523/JNEUROSCI.13-05-01852. 1993
- Warrant, E. J. (2008). Seeing in the dark: Vision and visual behaviour in nocturnal bees and wasps. *Journal of Experimental Biology*, 211(11), 1737–1746. http://doi.org/10.1242/jeb.015396
- Warrant, E. J. (2017). The remarkable visual capacities of nocturnal insects: Vision at the limits with small eyes and tiny brains. *Philosophical Transactions of the Royal Society B*, 372(1717), 20160063. http://doi.org/10.1098/rstb.2016.0063
- Warrant, E. J., & Dacke, M. (2011). Vision and visual navigation in nocturnal insects. *Annual Review of Entomology*, 56, 239–254.

- Warton, D. I., Wright, I. J., Falster, D. S., & Westoby, M. (2006). Bivariate line-fitting methods for allometry. *Biological Reviews*, 81(2), 259–291. http://doi.org/10.1017/S1464793106007007
- Zeil, J., Ribi, W. A., & Narendra, A. (2014). Polarisation vision in ants, bees and wasps. In G. Horváth (Ed.), Polarized light and polarization vision in animal sciences (pp. 41–60). Berlin, Heidelberg, Germany: Springer Berlin Heidelberg.

How to cite this article: Sheehan ZBV, Kamhi JF, Seid MA, Narendra A. Differential investment in brain regions for a diurnal and nocturnal lifestyle in Australian *Myrmecia* ants. *J Comp Neurol*. 2019;527:1261–1277. https://doi.org/10.1002/cne.24617